The EUMETSAT Network of Satellite Application Facilities

ROM SAF
Radio Occultation Meteorology

ROM SAF CDOP-2

Visiting Scientist Report 24:

Testing a new model for the residual ionospheric correction error in GPS radio occultation retrievals

Julia Danzer

Danish Meteorological Institute (DMI)
European Centre for Medium-Range Weather Forecasts (ECMWF)
Institut d'Estudis Espacials de Catalunya (IEEC)
Met Office (METO)

Ref: SAF/ROM/DMI/REP/VS/24
Issue: Version 1.0
Date: 02 Sep 2014

DOCUMENT AUTHOR TABLE

	Author(s)	*Function*	*Date*	*Comment*
Prepared by:	Julia Danzer	ROM SAF Visiting Scientist	07/14	
Reviewed by (Internal):	Sean Healy	ROM SAF Local Manager	08/14	
Approved by:	Kent B. Lauritsen	ROM SAF Project Manager	02/09/14	

DOCUMENT CHANGE RECORD

Issue/Revision	*Date*	*By*	*Description*
Draft 1	06 May 2014	JD	Intermediate Report
Version 0.0	26 May 2014	JD	Final version intermediate report
Draft 1	30 June 2014	JD	First version end report
Version 1.0	02 Sep 2014	JD	Final version end report

VS Authors
This VS study was carried out by Dr. Julia Danzer, Wegener Center, Univ. of Graz, Austria; email: julia.danzer@uni-graz.at

VS Duration
The VS study was performed during March-July 2014 at the home institute of the candidate and with short visits to ECMWF during March 2014 and June/July 2014.

ROM SAF

The Radio Occultation Meteorology Satellite Application Facility (ROM SAF) is a decentralised processing center under EUMETSAT which is responsible for operational processing of GRAS radio occultation data from the Metop satellites and Radio Occultation (RO) data from other missions. The ROM SAF delivers bending angle, refractivity, temperature, pressure, and humidity profiles in near-real time and offline for NWP and climate users. The offline profiles are further processed into climate products consisting of gridded monthly zonal means of bending angle, refractivity, temperature, humidity, and geopotential heights together with error descriptions.

The ROM SAF also maintains the Radio Occultation Processing Package (ROPP) which contains software modules that will aid users wishing to process, quality-control and assimilate radio occultation data from any radio occultation mission into NWP and other models.

The ROM SAF Leading Entity is the Danish Meteorological Institute (DMI), with Cooperating Entities: i) European Centre for Medium-Range Weather Forecasts (ECMWF) in Reading, United Kingdom, ii) Institut D'Estudis Espacials de Catalunya (IEEC) in Barcelona, Spain, and iii) Met Office in Exeter, United Kingdom. To get access to our products or to read more about the ROM SAF please go to: http://www.romsaf.org.

Intellectual Property Rights

List of Contents

Executive summary

Radio Occultation (RO) sensing is used to probe the Earth's atmosphere in order to obtain information about its physical properties. When the radio signal passes through the atmosphere it experiences a phase shift, which is partly influenced by the due to solar radiation ionized part of the atmosphere. If the main interest are the atmospheric parameters of the neutral atmosphere, there is the need to correct for this ionospheric phase shift. Usually an ionospheric correction procedure is performed at bending angle level, which removes the ionospheric contribution to first order. Nevertheless ionospheric residuals remain, which affect the neutral atmospheric parameters.

In this study a new model for correcting the residual ionospheric error was tested. It is based on an integral expression for the residual error from the original paper of Vorobev and Krasilnikova. The model relates the residual error to the two GPS signals bending angles, $\alpha_1(a)$ and $\alpha_2(a)$, and furthermore to a coefficient $\kappa(a)$ dependent on impact altitude a.

The overall objective of this study was to explore the validity of the new residual ionospheric error model. In a first task a simulation study was set up, simulating day and night GPS RO profiles for the period of a solar cycle with and without ionosphere. The residual error was studied, the error model was tested, and temporal and spatial variations of $\kappa(a)$ were investigated. Furthermore, first tests of correcting bending angle data with the proposed ionospheric error model were conducted. The model performed well in the simulation study, capturing the temporal variability of the ionospheric residual. Although, it was not possible, due to high noise of the simulated bending angle profiles at mid to high latitudes, to perform a thorough latitudinal investigation of the performance of the model, first positive and encouraging results were found at low latitudes.

In a second study the proposed model was tested on observational GPS RO bending angle climatologies. The main goal in that study was to check for correlation between solar activity and the residual ionospheric error model, which should capture the temporal, solar cycle dependent evolution of the residual error. Correlation between the model and the solar activity could be detected, suggesting that the proposed model reduces residual ionospheric errors in climatological studies.

1 Introduction

The Radio Occultation (RO) technique gains information about the physical properties of a planetary atmosphere by detecting a change in a radio signal when it passes through this atmosphere. With the installment of the Global Positioning System (GPS) constellation this principle could be applied to scan the Earth's atmosphere. Using the GPS frequencies f_1 (1575.42 MHz) and f_2 (1227.62 MHz), the RO technique provides high quality profiles in the upper troposphere and lower stratosphere (UTLS) since 1995, see e.g., Kursinski et al. [9]. It has the advantage of all-weather capability, high-vertical resolution, and global coverage. The high data quality and long term stability make RO data suitable for climate applications.

The measured observable during an RO event are the phase delays of the transmitted electromagnetic signals L_1 and L_2, which are detected at a Low Earth Orbit (LEO) satellite. From the primary quantity phase delays bending angle profiles can be derived, from which, continuing in a processing chain, geophysical information such as, temperature or pressure, can be obtained. However, the signals total phase delays consists of neutral atmospheric phase delays as well as ionospheric phase delays. In order to be able to study the characteristics of the neutral atmosphere, the use of an ionospheric correction procedure is necessary. To first order it is possible to remove the ionospheric contribution, see, e.g., Spilker [19], Vorob'ev and Krasil'nikova [22], Ladreiter and Kirchengast [10], Syndergaard [21]. Nevertheless, higher order ionospheric residuals remain.

The dispersive nature of the ionosphere leads to differences in the bending of the two GPS signals f_1 and f_2. From a linear combination of the two signals the neutral atmospheric bending can be estimated. This linear combination removes the ionospheric contribution to first order and is commonly applied at all major processing centers at bending angle level [22].

The remaining residual ionospheric error is a function which varies with the 11 year solar cycle, being higher at day time compared to night time [3]. There is a reasonable concern on the impact of this residual ionospheric error on GPS RO level-3 products[1] [15]. The sensitivity of temperature level-3 products towards small bending angle biases has been tested within ROM SAF. Adding a bending angle bias of 0.05 μrad to an entire bending angle, resulted in an about 0.5 K difference at 30 km altitude in temperature. For comparison, solar maximum and day time conditions shows bending angle biases of about 0.3 μrad. This emphasizes the importance for a better understanding of residual ionospheric errors.

Residual ionospheric errors are often described as the omission of higher order magnetic terms in the ionospheric refractive index. It has been noted by Healy and Culverwell [7] that the research article by Vorob'ev and Krasil'nikova [22] contains an integral expression for the residual ionospheric error (Eq. 22), valid for a one-dimensional ionosphere with no magnetic field. First simulation tests of this expression showed that it produces residual errors comparable to errors in more complex simulations.

Healy and Culverwell performed simulations with a one-dimensional Chapman layer iono-

[1] ROM SAF level-3 products describe the monthly mean state of the atmosphere in the form of zonal averages, i.e. averages over all longitudes in 5-degree latitude bands. The range of data products includes both RO-specific variables (bending angle, refractivity) and common geophysical variables (temperature, humidity, pressure).

sphere, noticing there to be a simple relationship between the residual error and the L_1 and L_2 bending angles (residual ionospheric error model). This simple relationship has the potential to capture the problematic temporal variability of the residual ionospheric error.

In this study this new model for the residual ionospheric error is investigated, using both simulated and real data. In a first part the residual error model is tested for simulated data. RO events are simulated from 2001 until 2011, modeling according to the solar cycle a 3-dimensional non-spherical ionosphere through which the L_1 and L_2 signals pass. Furthermore co-located neutral atmospheric profiles are simulated. Monthly-mean residual ionospheric errors are computed, testing its temporal, as well as, spatial variability. The key question is if the proposed error model captures the simulated residual error as a function of time and space. In a second part real GPS RO monthly mean climatologies are used to study the correlation between the residual error model and the $F_{10.7}$ index.

The two studies should answer the question if the residual ionospheric error model is applicable to the more complex situation of a 3-dimensional non-spherical ionosphere, and finally, potentially to real observational GPS RO data.

2 Residual ionospheric error model

To first order the ionospheric corrected bending angle α_C is given by (using the formulation from Vorob'ev and Krasil'nikova [22])

$$\alpha_C(a) = \frac{f_1^2\alpha_1(a) - f_2^2\alpha_2(a)}{f_1^2 - f_2^2} \,, \tag{2.1}$$

where α_1 and α_2 are the f_1 and f_2 signal bending defined at the same impact parameter a (which is the perpendicular distance between one of the ray asymptotes and the center of refraction).

It is known that the magnitude of the residual ionospheric errors corresponds to the ionospheric electron density values, i.e., larger electron densities produce larger residual errors. Vorob'ev and Krasil'nikova [22] provide an integral expression for the residual ionospheric error $\Delta\alpha$, given for the case of a one-dimensional ionosphere with no magnetic field. This residual error depends on the vertical gradient of the square of the electron concentration (n_e^2), i.e.,

$$\Delta\alpha(a) \sim \int_a^\infty \frac{\left(\frac{d(n_e^2)}{dz}\right)}{(z^2 - a^2)^{3/2}} dz \,. \tag{2.2}$$

On the other hand, the ionospheric bending is related to the vertical integral of the gradient of electron density,

$$\alpha(a) \sim \int_a^\infty \frac{\left(\frac{d(n_e)}{dz}\right)}{(z^2 - a^2)^{1/2}} dz \,. \tag{2.3}$$

This suggests a relationship between the two. Healy and Culverwell calculated the residual ionospheric error for the case of a Chapman layer ionosphere. The residual error $\Delta\alpha$(a) as a function of impact parameter a is then described by

$$\Delta\alpha(a) = \alpha_C(a) - \alpha_N(a) = -\kappa(a)(\alpha_1(a) - \alpha_2(a))^2 \,, \tag{2.4}$$

with α_C [rad] being the to first order ionospheric corrected bending angle (see Eq. 2.1) and α_N [rad] being the neutral atmospheric bending angle. This simple expression for the residual error is the key formula in this study. From calculations the factor $\kappa(a)$ [rad^{-1}] is found to be a simple function of the impact parameter, the peak height of the Chapman layer and its width [7]. Healy and Culverwell performed a first time simulation with a one-dimensional Chapman layer, where $\kappa(a)$ seemed to be a slowly varying function of impact altitude (defined as impact parameter minus radius of curvature minus geoid undulation). This implies that the temporal variability of the residual error is might captured by the $(\alpha_1 - \alpha_2)^2$ [rad^2] term. Given the potential improvements on GPS RO level-3 data products, Eq. 2.4 needs to be investigated for more complex situations.

Our analysis starts with the simulation study, having the advantage that the residual error can directly be calculated. RO events were simulated with and without ionosphere, making it possible to calculate the difference between the ionospheric corrected bending angle α_C (simulations with ionosphere) and the neutral bending angle α_N (simulations without ionosphere) at same time and space. Calculating also the $(\alpha_1 - \alpha_2)^2$ term enables to study the

coefficient κ, dependent on time (11 year period), impact altitude a, and space (latitudinal dependance). If the proposed model for the residual ionospheric error captures the temporal variability of the residual error, κ should be almost constant with time. After κ has been assessed, a first bending angle correction using the residual error model is performed. Its impact is then studied on temperature profiles (see Sec. 4.4).

Finally the error model is tested on real GPS RO data by studying 30° zonal monthly averages of $(\alpha_1 - \alpha_2)^2$ as a time series over the period of about one solar cycle. Furthermore the correlation of the term $(\alpha_1 - \alpha_2)^2$ to the solar activity ($F_{10.7}$ index) is analyzed.

3 Data sets

3.1 Simulated data

With the EGOPS software (End-to-End Generic Occultation Performance and Processing System) version 5.5 [5] I performed an End-to-End simulation study, simulating day (12:00 and 15:00, local time) and night time (02:00, local time) profiles, similar to the study in Danzer et al. [3]. The profiles were simulated for the years 2001 to 2011 via ray tracing through ionospheric and neutral atmospheric fields. During the simulations the neutral atmosphere was held constant, while the ionosphere was varied for each profile. For the constant neutral atmosphere I used an operational analysis field provided by the ECMWF (European Centre for Medium-Range Weather Forecasts) from 1 January 2007 with T42L91 resolution. The horizontal resolution T42 corresponds to the resolution of RO data (300 km), with data available at 91 vertical levels (L91).

The non-spherical 3D dimensional ionosphere was simulated with the NeUoG model from the University of Graz [12, 11]), which is driven by the $F_{10.7}$ index as an indicator for the solar activity. The $F_{10.7}$ index is based on the solar radio flux at a wavelength of 10.7 cm. The $F_{10.7}$ data, given on a daily basis, has been downloaded from the website of the National Oceanic and Atmospheric Administration, NOAA (`ftp://ftp.ngdc.noaa.gov/STP/SOLAR_DATA/SOLAR_RADIO/FLUX/Penticton_Observed/daily/DAILYPLT.OBS`, 2012). I produced events taking place in all Januaries from 2001 to 2011 at latitude band 0°, 5°S/N, 10°S/N, continuing in 10° steps until 60°S/N. Each latitude between 10°S/N was simulated at 12 different longitudes in 30° steps, above 10°S/N 60° steps were used.

Furthermore I simulated neutral atmospheric events, employing the same ECMWF analysis field from 1 January 2007, studied at the respective geographic locations, i.e., 0°, 5°S/N, 10°S/N, continuing in 10° steps until 60°S/N, at 12 different longitudes, and above 10°S/N simulating 60° longitude steps.

In this study the ionospheric corrected bending angle α_C, the L_1 and L_2 bending angles α_1 and α_2, as well as the neutral atmospheric bending angle α_N were analyzed. Extremely noisy events were rejected as outliers, using in an altitude range between 50 km to 80 km a threshold of $\pm 7\,\mu$rad in difference to the respective neutral atmospheric bending angle at same occultation location, following the suggestion of Liu et al. [14]. Although no detailed study on the percentage of rejected profiles was performed, random sampling showed a reduction of about 5 %, which is in line with results from Liu et al. [14]. The bending angle profiles were studied as mean profiles averaged over all longitudes within a latitude band, studied separately for day and night. Additionally the following zonal climatologies were tested: 5°S to 5°N, 10°S to 10°N, 10°S to 30°S, 10°N to 30°N, 30°S to 60°S and 30°N to 60°N.

3.2 Satellite data

In order to test the ionospheric error model on observational data for the time period of about one solar cycle, I used GPS RO (Global Positioning System Radio Occultation) data from the CHAMP (Challenging Mini–Satellite Payload) and COSMIC (Constellation Observing System for Meteorology) satellite missions. Excess phase profiles and precise orbit information were retrieved from the UCAR/CDAAC (University Corporation for Atmospheric Research/Cosmic Data Analysis and Archive Center) database and further processed with the EGOPS software version 5.6. CHAMP data were studied from July 2001 until December 2006, COSMIC data were studied from January 2007 until December 2012. COSMIC data were analyzed on a monthly basis, for CHAMP data a three months moving average was used, due to the reduced number of profiles for the single satellite mission. Furthermore the data were processed to 30° zonal climatologies, using the CLIPS2 (Climatology Processing System 2) software, distinguishing day and night local time frames. Profiles between 11:00 to 15:00 local time were took as a representative for day time, profiles between 02:00 to 06:00 represented night time.

In the satellite data study the key observable of interest was the term $(\alpha_1 - \alpha_2)^2$. The quantity was studied as a time series from the years 2001 until 2012. Furthermore the observables correlation to the solar activity, i.e., the $F_{10.7}$ index, was tested. The $F_{10.7}$ index is given in [sfu] (solar flux unit), where 1 sfu = $10^{-22}\mathrm{Wm}^{-1}\mathrm{Hz}^{-1}$. For the $F_{10.7}$ index data were taken from the website of the Industrial Plant & Service (IPS) Australia, under `http://www.ips.gov.au/Solar/1/6`. They provide smoothed monthly data using a 13 monthly running filter (first and last half weighting), where all solar radio flux values were obtained from sunspot numbers using a statistical conversion.

4 Simulation study

4.1 Initial bending angle analysis

As a primary investigation single day and night time bending angle (BA) profiles α_C were systematically studied for different latitude bands, as a function of impact altitude. As an example, Fig. 4.1 shows all simulated bending angle profiles between the latitude band 5°S to 5°N, giving a first impression of the sometimes bad bending angle quality (top). In the bottom plot outliers $\pm 7\,\mu$rad were rejected, reducing the number of day profiles (orange) from 383 down to 367, and the number of night profiles (blue) from 341 down to 340. The red line shows the mean neutral atmospheric bending angle profile between 5°S to 5°N. Analyzing bending angle profiles for other latitude bands showed, that towards higher latitudes the number of extremely noisy events increases.

In general, in the following series of plots the day time profiles are color schemed in warm colors, while the night time profiles are color schemed in cold colors. As a start, I decided to investigate initially only the latitude band 0°. The residual bending angle error $(\alpha_C - \alpha_N)$ is a function of impact altitude a. Since we are interested in the change of this error dependent on solar activity, I studied the mean day time and night time residual error for each year from 2001 until 2011, dependent on impact altitude, see Fig. 4.2. This plot is extremely illustrative, since it already exhibits possible problems in the analysis. The residual bending angle error shows dominantly a value of about $\pm 0.5\,\mu$rad (depending on impact altitude), fluctuating strongly at each impact altitude, sometimes also in the same range of value ($\sim 0.5\,\mu$rad). Hence, when we will study the coefficient κ according to Eq. 2.4, we will face problems with the magnitude of the noise, which is in a similar range as the residual error itself. Surprisingly also the night time residual error shows rather large fluctuations. Nevertheless, one can observe a clear tendency of an increasing residual error at day time in the years of high solar activity, such as 2001 and 2002, reducing to smaller values in the years of low solar activity, such as 2007 and 2008.

In Fig. 4.3 the mean residual error is studied as a time series for each year from 2001 until 2011, at three fixed impact alitudes, comparing night and day time profiles. Since the residual error fluctuates strongly for each year and impact altitude, as shown in Fig. 4.2, the expected increase of the residual error in the years of high solar activity can not be detected. Studying in Fig. 4.4 the function $(\alpha_1 - \alpha_2)^2$ as a time series at fixed impact altitudes we find for night and day time an increase of the magnitude of this function in the years of high solar activity. During the day this increase is naturally higher than during the night. This result suggests that the temporal variability in the residual error might be determined by the $(\alpha_1 - \alpha_2)^2$ term.

Finally, I show in Fig. 4.5 a scatter plot of the residual error versus the $(\alpha_1 - \alpha_2)^2$ term for single profiles simulated at 0° latitude, studied at the three impact altitudes 50 km, 60 km, and 70 km. The dependance between those two terms counts to the key relation of this study. Ideally the two terms $(\alpha_C - \alpha_N)$ versus $(\alpha_1 - \alpha_2)^2$ show a straight line, where the fitting coefficient assigns κ. In this plot we already see that due to noise the single profiles scatter over about 1 μrad, which makes it difficult to evaluate the fitting coefficient $\kappa(a)$. Especially the night time profiles show rather large noise. The magnitude of the noise seems to be similar to the magnitude of the observable. This affects night time profiles even stronger since due to the smaller values of the observable the noise has a larger impact. In the next section I discuss how in this study the noise problem in the data will be handled.

4.2 Vertical averaging of bending angle profiles

In the research article by Danzer et al. [3] the bending angle bias is studied as the difference between the observed or simulated bending angle and the co-located bending angle of the MSIS (Mass Spectrometer and Incoherent Scatter Radar) climatology, averaged over an altitude range between 65 km to 80 km. The bending angle bias, studied separately for day and night profiles, illustrates nicely the increase of the day time bias due to residual ionospheric errors in the bending angle data, especially in the years of high solar activity. In this study we are interested on the dependance of the coefficient $\kappa(a)$ on impact altitude, as well as time and space. Similar to the just described study, we decided to perform a vertical averaging of the quantities $\alpha_C(a)$, $\alpha_1(a)$, and $\alpha_2(a)$. The observables were averaged at each impact altitude grid point over an altitude range of 5 km, between 10 km to 75 km. The vertical averaging smoothes the bending angles and respectively, the two terms $(\alpha_C - \alpha_N)$ and $(\alpha_1 - \alpha_2)^2$, without losing the information of impact altitude.

Fig. 4.6 shows, exactly as in Fig. 4.2, the residual bending angle error $(\alpha_C - \alpha_N)$ dependent on impact altitude a, for mean day and night time profiles from 2001 until 2011. In contrast to Fig. 4.2, the bending angle data was vertically averaged at each impact altitude. Obviously the residual error is much smoother than before, suggesting that a study of the residual error dependent on time now might be possible.

In the top plot of Fig. 4.7 the residual error is studied dependent on time, for mean night and day time bending angle profiles at fixed impact altitudes. Similar to the results of the bending angle bias study by Danzer et al. [3], the night time residual error stays constant over time, while the day time residual error increases in the years of high solar activity. The bottom plot shows a scatter plot of this mean residual error $(\Delta\alpha)$ versus the $(\alpha_1 - \alpha_2)^2$ term. Compared to the previous scatter study this time the noise is reduced, and data fitting, using the method of least squares, was possible. I tested the least square method by using day and night profiles together for the regression analysis (blue solid lines), as well as, only day profiles (orange solid lines). The plot also shows the value of the resulting fitting coefficient κ dependent on impact altitude a (given in [rad^{-1}]), including and excluding night profiles in the fitting[1]. The values for κ are in good agreement with estimated values of κ from calculations [7].

[1] Note that the values for the coefficient κ are negative in Fig. 4.7. The reason is that the minus sign from Eq. 2.4 has not been taken into account in this analysis.

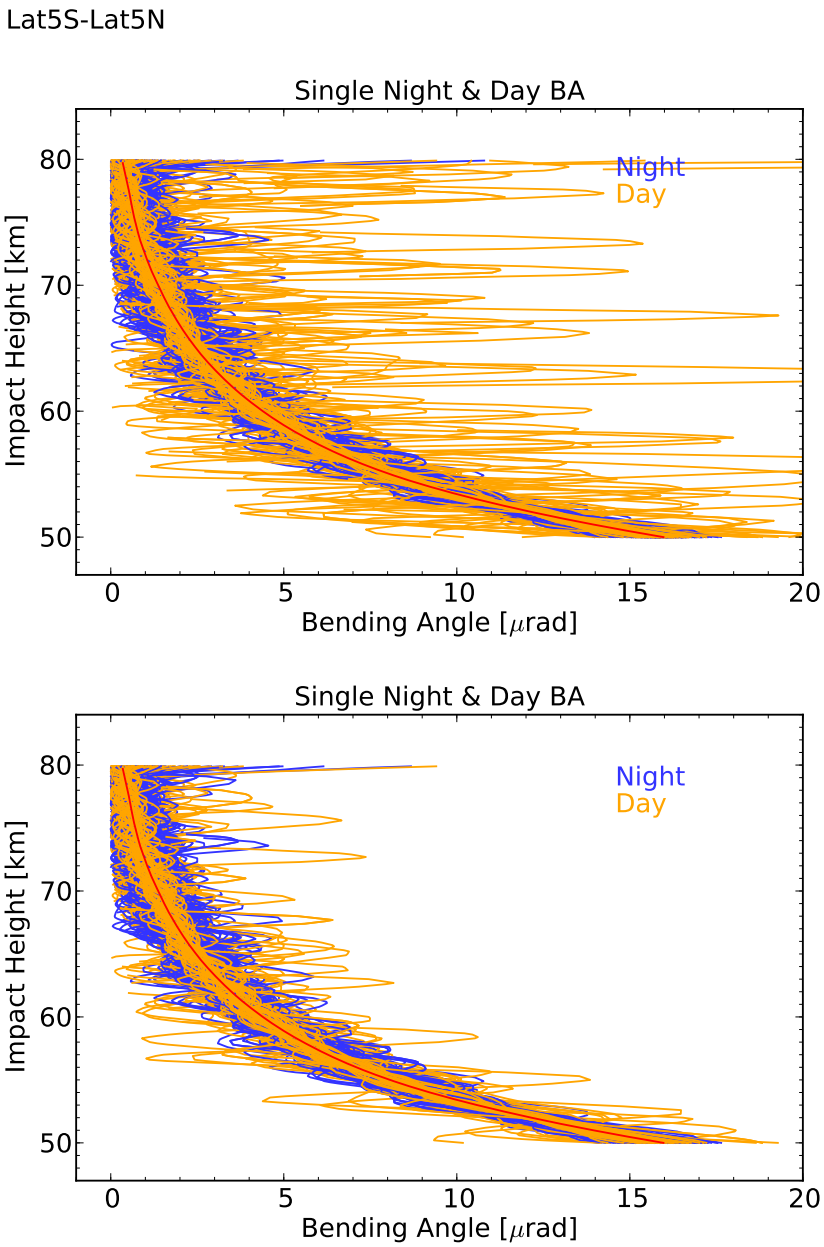

Figure 4.1: *Single day and night time bending angle profiles, with (bottom) and without (top) outlier rejection.*

Lat0

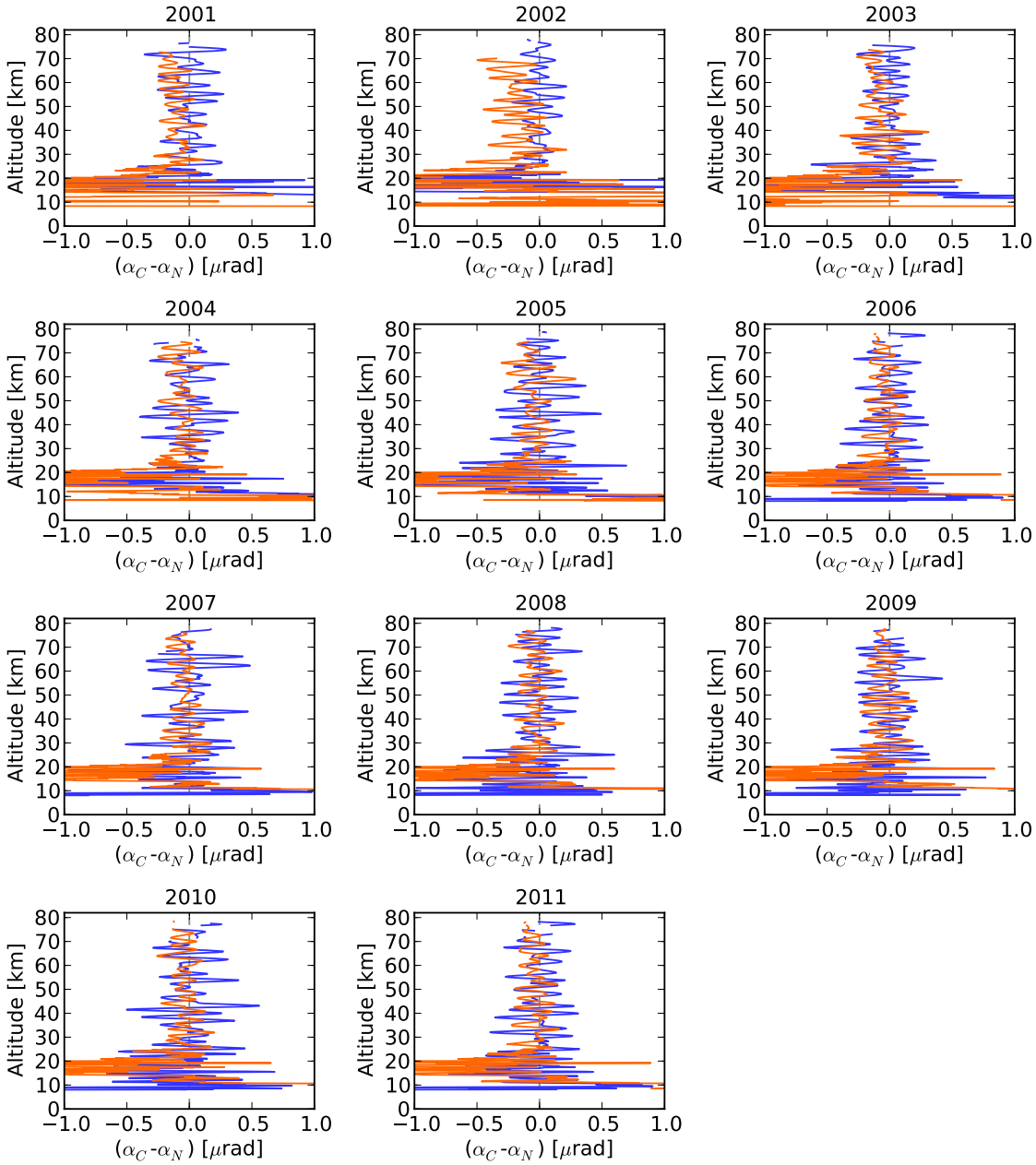

Figure 4.2: *Residual bending angle error dependent on impact altitude for mean night (blue) and day time (orange) profiles at* 0° *latitude, studied from* 2001 *until* 2011.

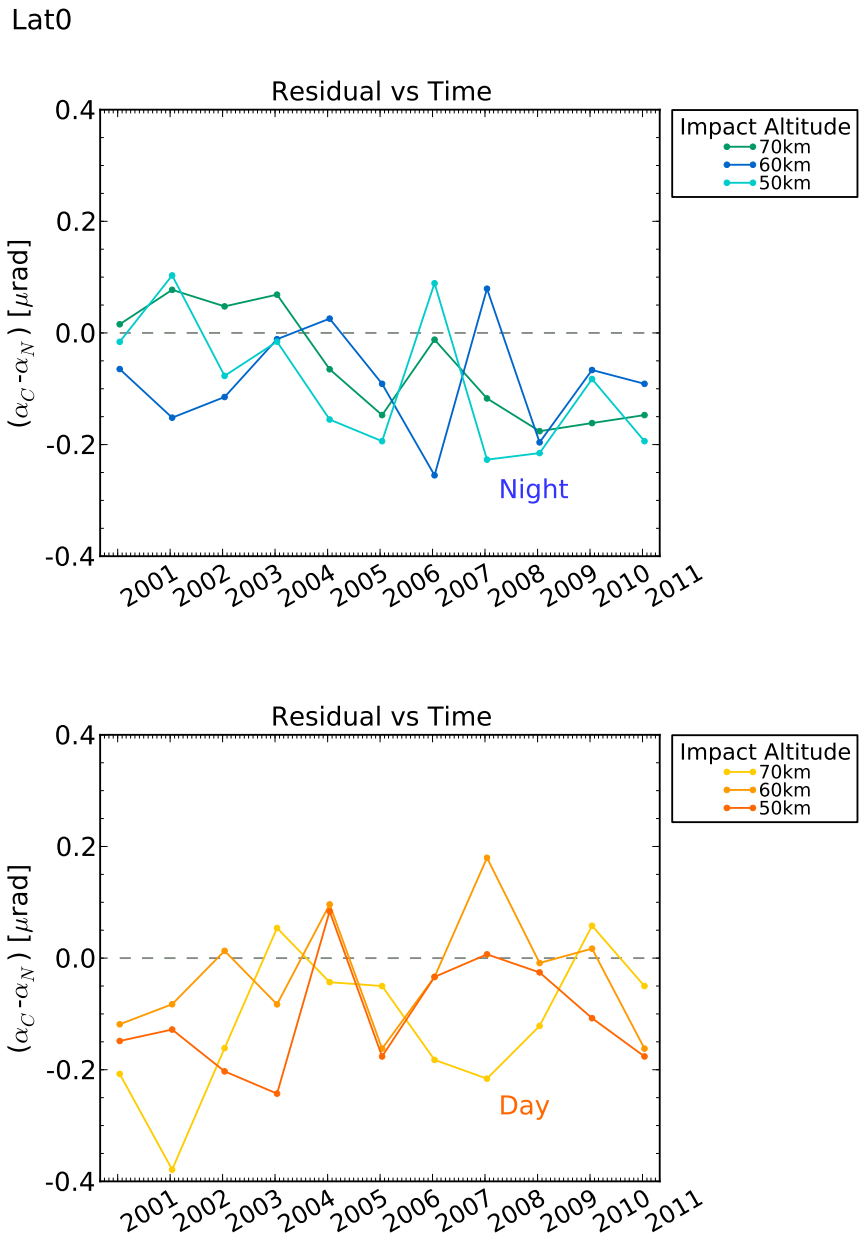

Figure 4.3: *Time series of night (top) and day time (bottom) mean residual bending angle error, illustrated for* 0° *latitude, studied for the three impact altitudes* 50 km, 60 km, *and* 70 km.

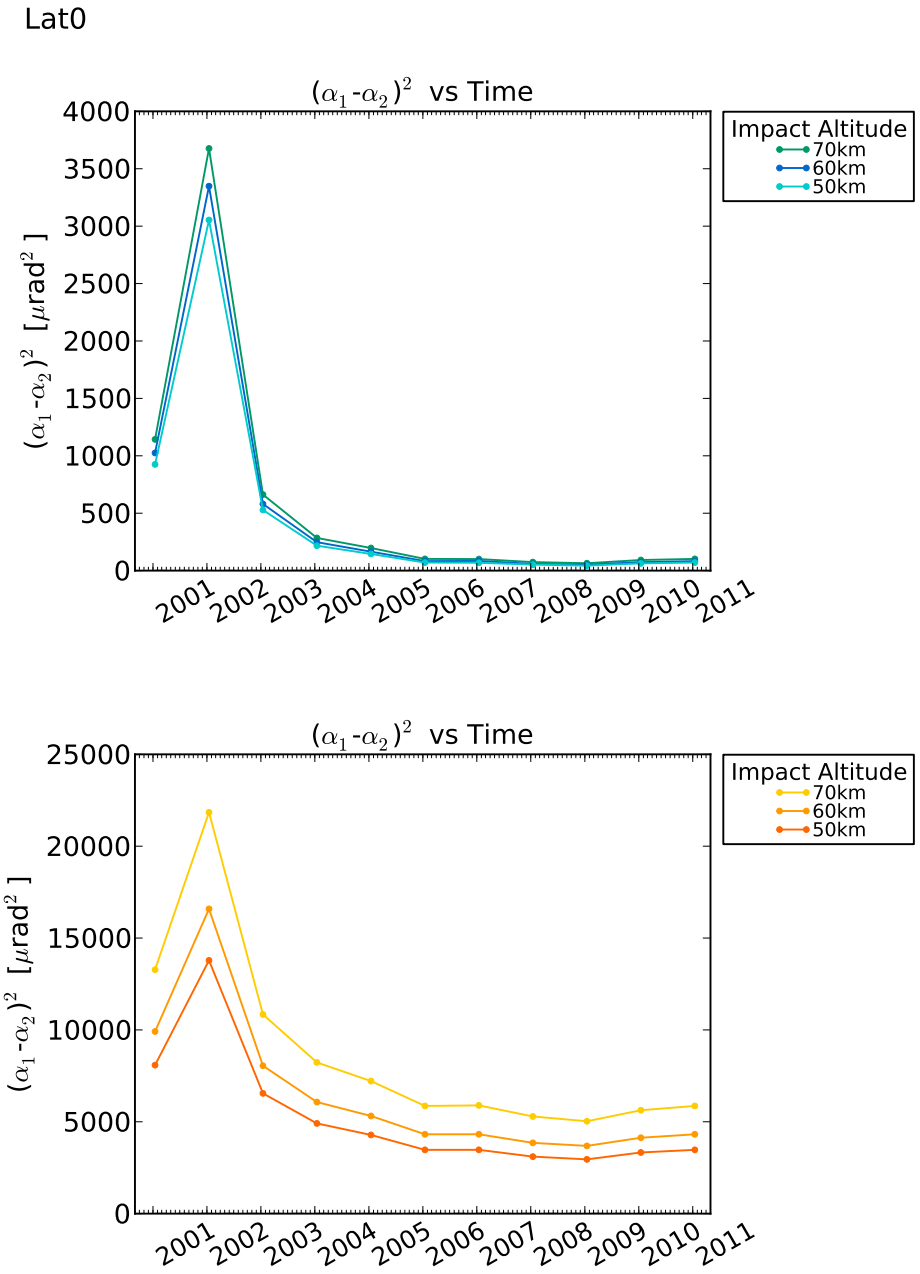

Figure 4.4: *Time series of night (top) and day time (bottom) mean* $(\alpha_1 - \alpha_2)^2$*, illustrated for* 0° *latitude, studied for the three impact altitudes* 50 km*,* 60 km*, and* 70 km*.*

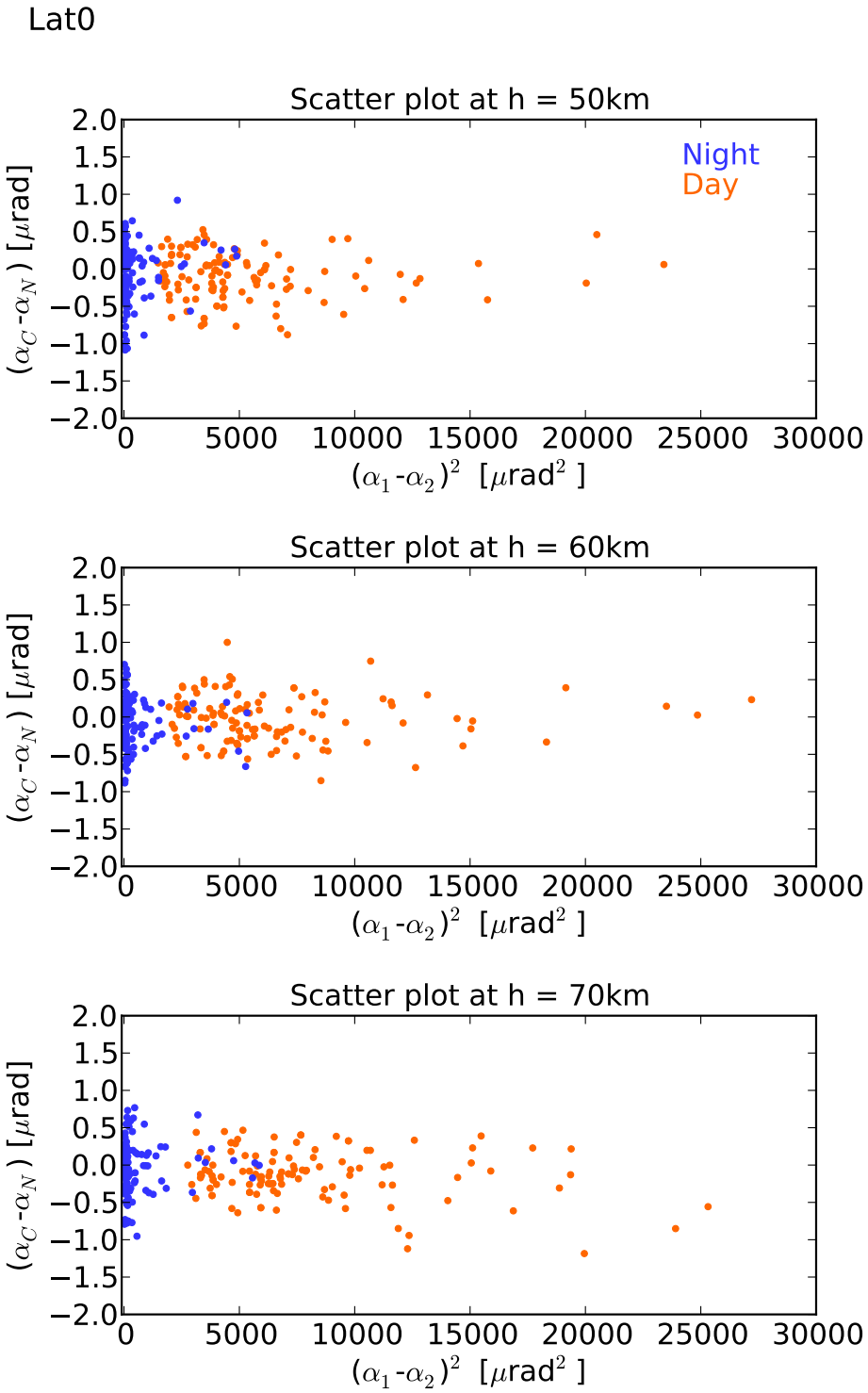

Figure 4.5: *Scatter plot of night and day time bending angle residual versus* $(\alpha_1 - \alpha_2)^2$ *for all single bending angle profiles at latitude* 0°*, studied at the three impact altitudes* 50 km*,* 60 km*, and* 70 km*.*

Finally $\kappa(a)$ is analyzed in Fig. 4.8 as a function of time, for three fixed impact altitudes for day time conditions. κ was determined by analyzing $(\alpha_C - \alpha_N)/(\alpha_1 - \alpha_2)^2$ for each year, at latitude 0°. Obviously for day time conditions $\kappa(a)$ shows to be maximally a value between about $0\,\mathrm{rad}^{-1} < \kappa(a) < 20\,\mathrm{rad}^{-1}$ for each year, being more or less constant with time, fluctuating around a mean value of about $\kappa(a) = 14\,\mathrm{rad}^{-1}$. Hence, we can assume that $(\alpha_1 - \alpha_2)^2$ catches the temporal variability of the residual ionospheric error. Studying night time conditions (not shown), the larger impact of the noise prohibits a similar nice result and $\kappa(a)$ fluctuates in a much broader range of values.

4.3 Systematic study of the coefficient κ

In this section $\kappa(a)$ is studied dependent on impact altitude, for different latitude bands and zonal averaging. As a primary analysis Fig. 4.9 shows $\kappa(a)$ for latitude band 0°. The coefficient κ was determined with the least square method as shown in the bottom plot of Fig. 4.7, applied on each impact altitude separately. The l.h.s. of Fig. 4.9 shows the complete function $\kappa(a)$, while the r.h.s. shows only the range from 30 km to 80 km altitude. Below 30 km altitude $\kappa(a)$ could not reliably be determined. Within this altitude range $\kappa(a)$ shows values between $5\,\mathrm{rad}^{-1}$ to $20\,\mathrm{rad}^{-1}$, where below 50 km altitude fluctuations start to increase.

Unfortunately, a reliable study on the dependance of κ on latitude was not possible due to large fluctuations in the data. We had to concentrate on low latitudes, where the results are shown in Fig. 4.10. The top plot shows κ studied for single latitude bands, while the bottom plot compares zonal averaging. The single latitude bands are studied from 10°N to 10°S, ranging from values for κ between about $\kappa(a) = -20\,\mathrm{rad}^{-1}$ to $\kappa(a) = 30\,\mathrm{rad}^{-1}$. It is noticeable that northern latitudes show in this study the tendency to lower κ values compared to southern latitudes. This could be due to simulating southern hemisphere summer conditions. Personally I think, in order to perform a serious latitudinal study, a larger ensemble setup needs to be evaluated. In this study the occultation plane was chosen from north to south for every occultation event, which also produces a selection effect for an event. Varying the occultation plane produces a larger diversity in the events, whereas choosing always the same occultation plane simulates at a nearby location most likely a very similar event. If this event is of bad bending angle quality, or odd in any kind of way, it can get simulated several times. To reduce this selection effect I also studied zonal bands, and tested different zonal averaging, see bottom plot of Fig. 4.10. This shows a larger consistency between the κ values at low latitudes. I also included a zonal band between 30°S to 10°N, which is the equatorial day time region, due to simulating southern conditions.

Although the simulation study faced some problems, such as noise and bad bending angle quality at higher latitudes, it could present some first encouraging results. Clearly, a correlation between the residual ionospheric error and the $(\alpha_1 - \alpha_2)^2$ term could be shown. First positive results, supporting Eq. 2.4 have been presented. In the last section of this chapter the correction will be tested on bending angle data.

Lat0

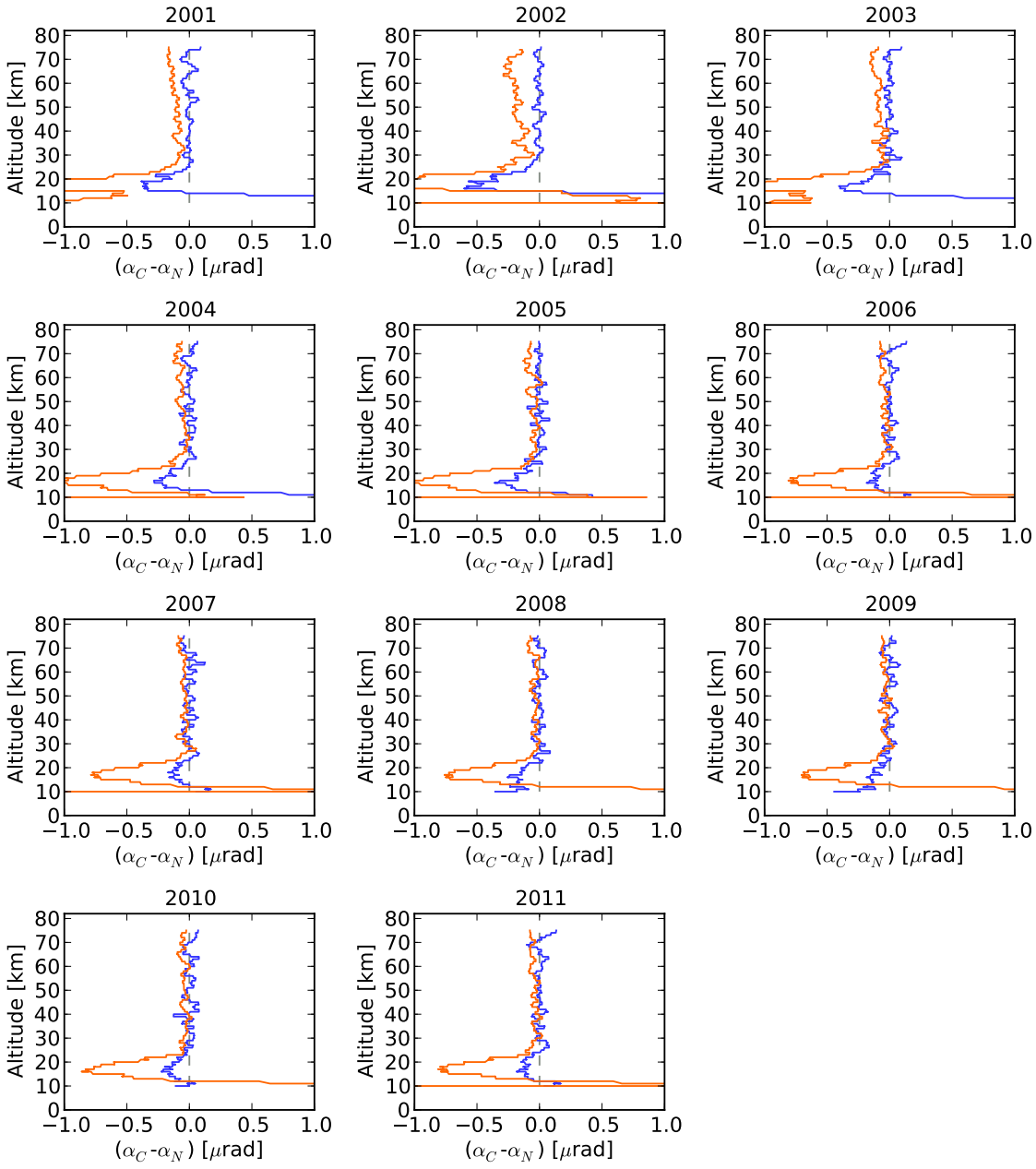

Figure 4.6: *Residual bending angle error dependent on impact altitude for mean night (blue) and day time (orange) profiles at* 0° *latitude, studied from* 2001 *until* 2011. *At each impact altitude a vertical averaging over* 5 km *was applied.*

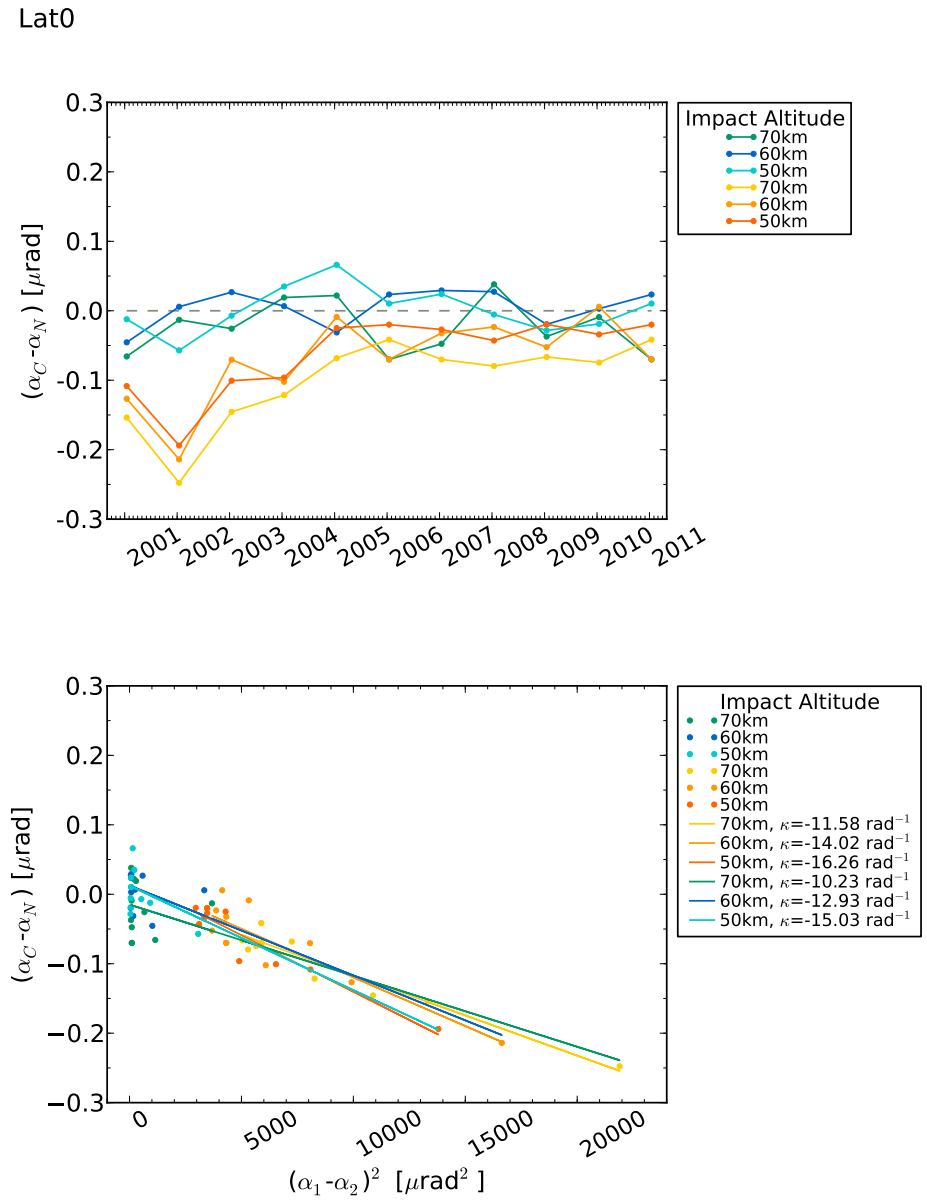

Figure 4.7: *The top plot shows the vertically averaged residual night and day time bending angle error dependent on time, while the bottom plot shows the scatter plot of the residual error versus* $(\alpha_1 - \alpha_2)^2$*, studied on three impact altitudes and on latitude* $0°$*.*

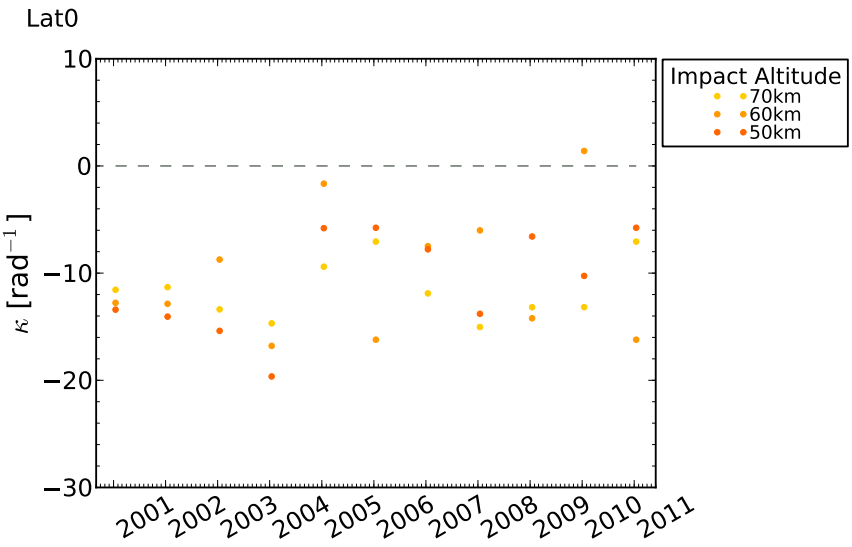

Figure 4.8: *The coefficient κ dependent on time for day time profiles at latitude 0°, studied for three impact altitudes.*

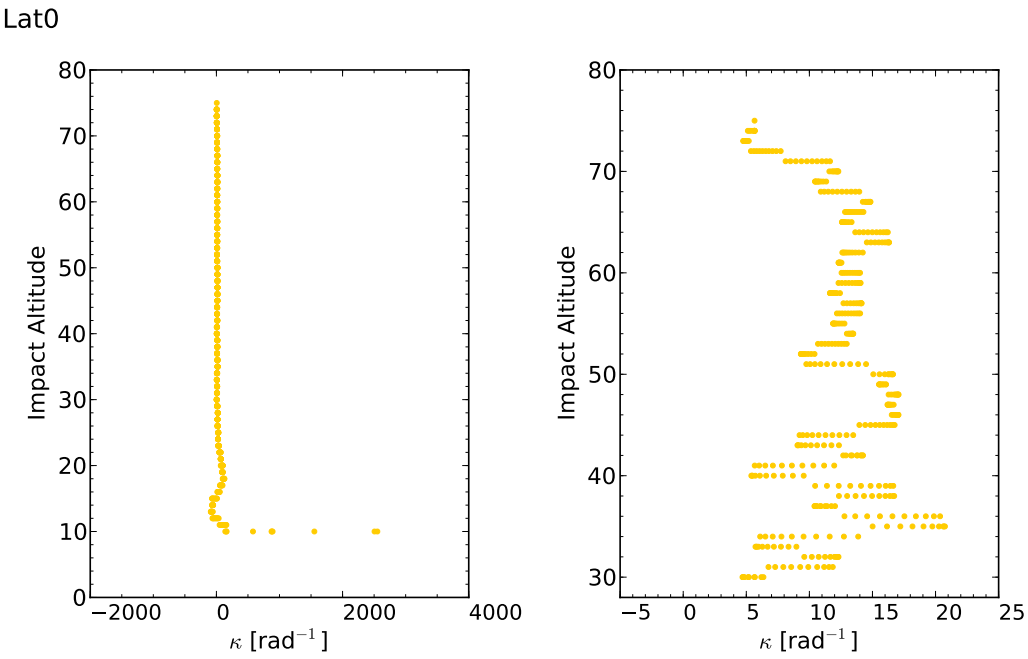

Figure 4.9: *The coefficient κ dependent on impact altitude a, plotted for latitude band 0°.*

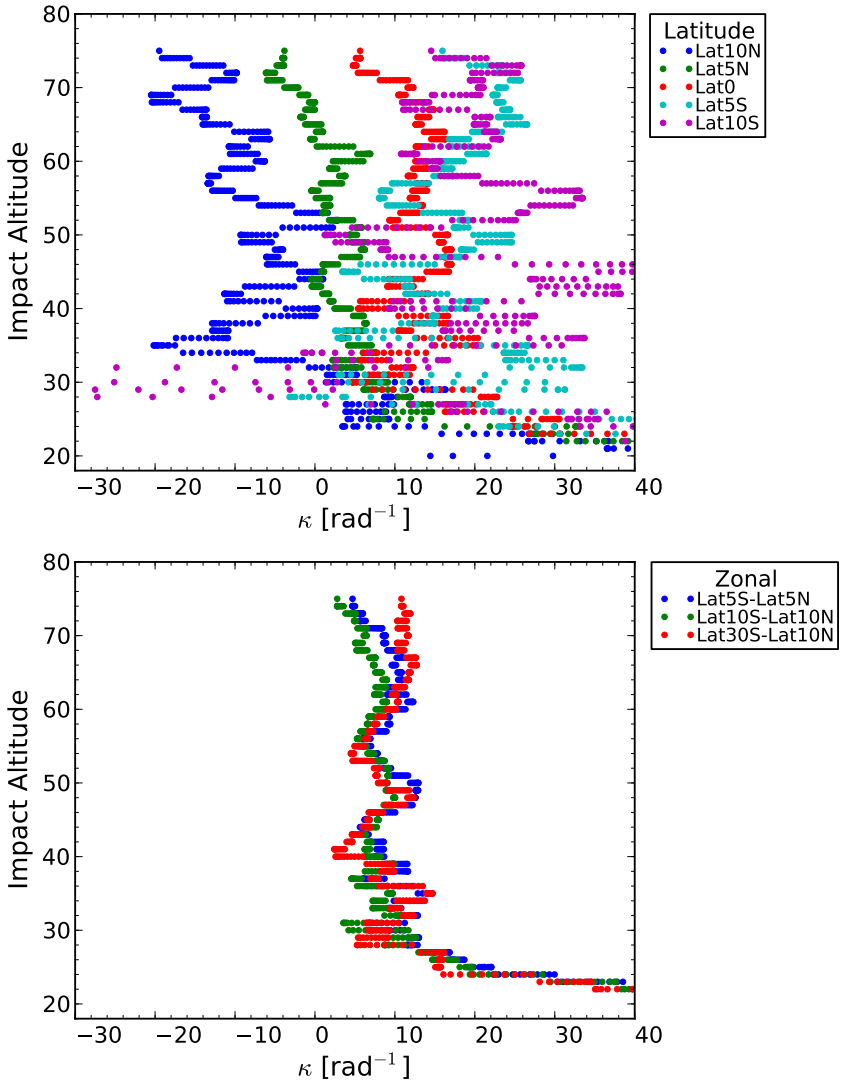

Figure 4.10: *The coefficient κ dependent on impact altitude, plotted for different latitudes (top plot) and zonal climatologies (bottom plot).*

4.4 Testing the residual ionospheric correction

In this section temperature profiles, simulated at 0° latitude and longitude were studied from 2001 until 2011. The profiles were simulated with different values of the $F_{10.7}$ index, according to the solar activity in this period of time. Furthermore, the same data set was reproduced, applying the **res**idual **i**onospheric **c**orrection (RESIC) on the bending angle data, i.e., the neutral atmospheric bending angle was found by

$$\alpha_N(a) = \alpha_C(a) + \kappa(a)(\alpha_1(a) - \alpha_2(a))^2 \ . \tag{4.1}$$

The l.h.s. of Fig. 4.11 shows the difference between the temperature profiles simulated without RESIC and the neutral gas temperature field (1 January 2007) in an altitude range between 10 km to 35 km, from 2001 until 2011. Profiles simulated with highest solar activity, such as 2001 and 2002, show largest temperature differences, with a maximum value of about 2 K for 2002 at 35 km altitude. As expected, temperature differences towards the neutral gas field decrease for lower solar activity. The r.h.s. of Fig. 4.11 shows temperature differences where RESIC was applied on the simulated bending angle data, according to Eq. 4.4. The four values $\kappa(a) = 10\,\mathrm{rad}^{-1}$, $\kappa(a) = 14\,\mathrm{rad}^{-1}$, $\kappa(a) = 16\,\mathrm{rad}^{-1}$ and $\kappa(a) = 20\,\mathrm{rad}^{-1}$ were tested. In this initial study κ was applied on the bending angle data as a constant factor with no dependance on impact altitude a. The dependance on impact altitude enters only from $\alpha_C(a)$, $\alpha_1(a)$, and $\alpha_2(a)$. Obviously, for the highest value of $\kappa(a) = 20\,\mathrm{rad}^{-1}$ best results were achieved, leading to smallest temperature differences, i.e., closest values to the simulated neutral atmosphere profile.

This initial test study showed that residual ionospheric errors are reduced when applying RESIC. Even when κ is applied as a constant factor data quality improves and values closer to the neutral atmosphere profile are retrieved. This supports the assumption that the temporal variability of the residual error $(\alpha_C - \alpha_N)$ is at least partly captured by the $(\alpha_1 - \alpha_2)^2$ term.

In Fig. 4.12 the magnitude of the residual ionospheric correction is compared to the computed residual ionospheric error, studied at latitude band 0° and for day time profiles. From previous studies we know that for the simulated data at latitude band 0°, κ is in the order of $\kappa(a) = 14\,\mathrm{rad}^{-1}$, see e.g. Fig 4.7 and Fig 4.9. The residual error (calculated as 5 km vertically smoothed average) is studied dependent on altitude, separately for each simulated year. The residual ionospheric correction is computed with RESIC, i.e., $\kappa(\alpha_1(a) - \alpha_2(a))^2$, using the retrieved value $\kappa(a) = 14\,\mathrm{rad}^{-1}$ from calculations, and for testing reasons, an arbitrary $\kappa(a) = 30\,\mathrm{rad}^{-1}$. Obviously, using the value $\kappa(a) = 14\,\mathrm{rad}^{-1}$ from calculations (blue line) very well matches the computed residual ionospheric error, concluding the residual ionospheric error model delivers the residual error close to the actual value. However, when using an arbitrary value of κ, a wrong magnitude of the residual error is computed, where in that chosen case the residual error is overestimated (green line). From this study we can learn two things. On the one hand RESIC seems to produce the residual ionospheric error. On the other hand, a very thorough study of the value κ needs to be performed. This will be discussed in detail in the Summary and Discussion Sec. 6.

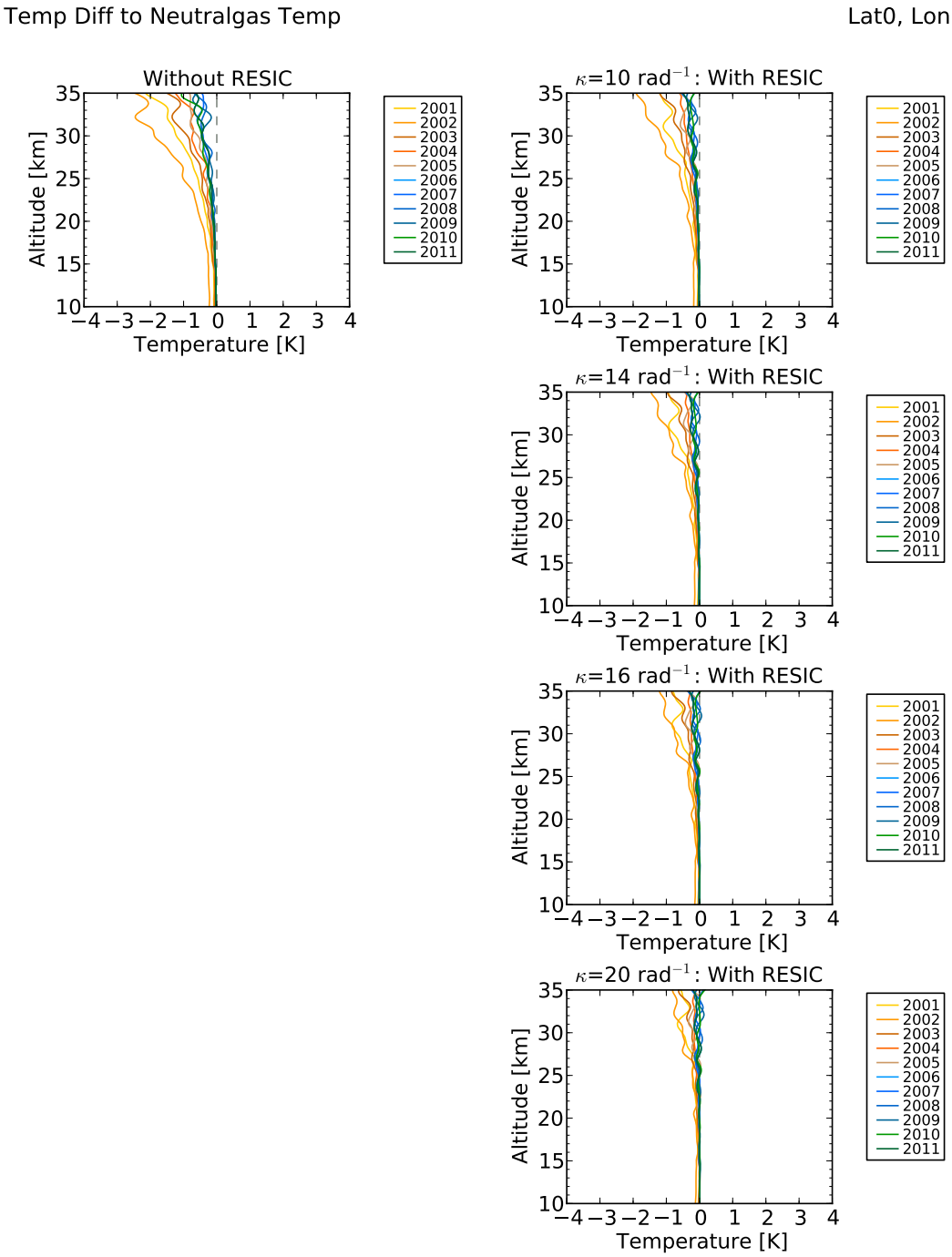

Figure 4.11: *Studying the effect of the residual ionospheric correction on temperature profiles, studied for different values of κ.*

Finally, once again the residual ionospheric correction is studied on temperature profiles. This time RESIC is studied for the latitude band 0°, instead of on a single profile. The correction is applied on all day time profiles within this latitude band, using the retrieved value $\kappa(a) = 14\,\mathrm{rad}^{-1}$ for the correction. Fig. 4.13 shows the mean temperature profiles, simulated with different solar activity for each year, relative to the neutral temperature profile. On the l.h.s. the temperature difference is studied without RESIC up to 50 km, while on the r.h.s. RESIC has been applied. Clearly when applying the correction the results improved, and values closer to the neutral temperature were achieved. The relative temperatures show to be a narrow bunch around zero, with only the exception of the mean profile for the year 2002. This result further encourages the proposed residual ionospheric correction model, but also shows the importance of studying the coefficient κ very thoroughly.

With this last plot I close the simulation study concluding that some first positive and encouraging results supporting the proposed residual ionospheric error model were found. It could be shown that the temporal variability of the residual error is captured by the $(\alpha_1(a) - \alpha_2(a))^2$ term, and that the coefficient κ is a constant value with time. Furthermore, applying the proposed correction on the bending angle data achieved results closer to the neutral atmosphere profiles. However, at that point also some limits of this study could be detected. It was not possible to perform a latitudinal study of the coefficient κ, due to high noise in the simulated data.

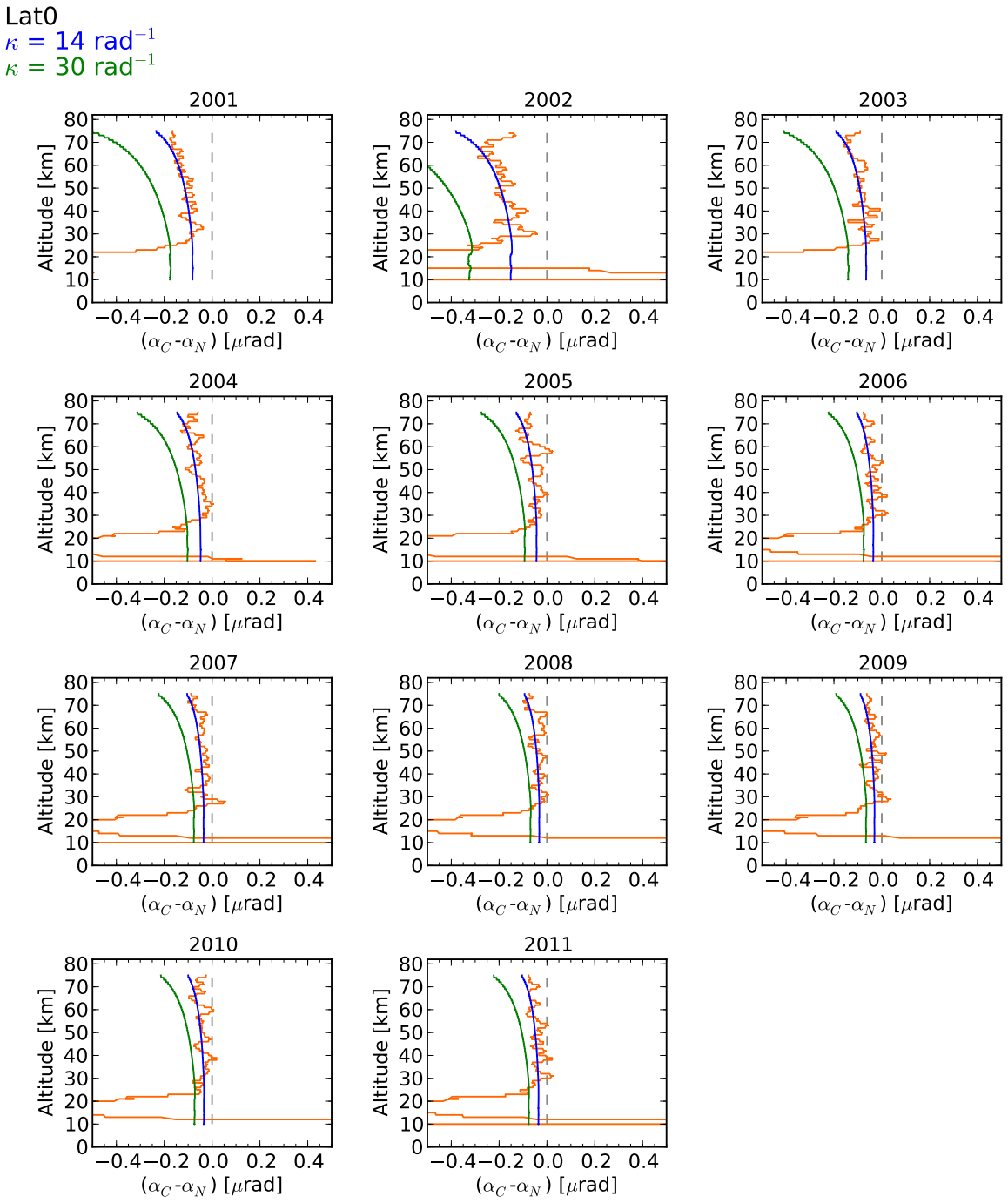

Figure 4.12: *Comparing the residual ionospheric correction to the monthly mean day time residual error at latitude band* $0°$*, choosing* $\kappa(a) = 14\,\mathrm{rad}^{-1}$ *(blue) and* $\kappa(a) = 30\,\mathrm{rad}^{-1}$ *(green) in the correction model.*

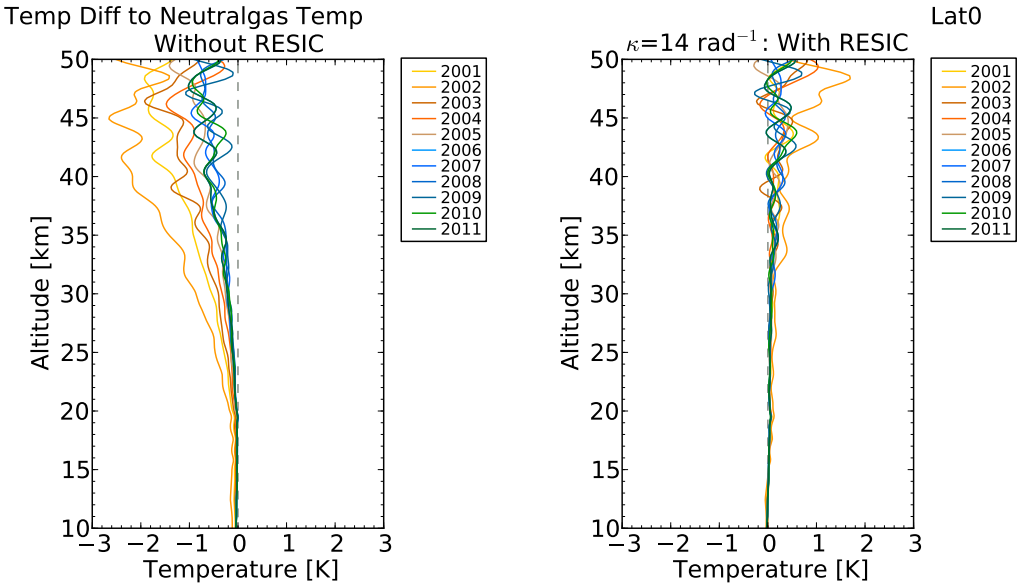

Figure 4.13: *Testing the effect of the residual ionospheric correction on temperature profiles, studied for latitude band* $0°$ *and using the coefficient* $\kappa(a) = 14\,\mathrm{rad}^{-1}$ *from calculations.*

5 Satellite data study

5.1 Initial analysis

In this study CHAMP and COSMIC satellite data have been binned to 30° zonal monthly climatologies and were analyzed from the years 2001 up to 2012. We start the analysis with investigating the primary quantity of interest, i.e., the term $(\alpha_1(a) - \alpha_2(a))^2$.

Fig. 5.1 shows the time series of $(\alpha_1(a) - \alpha_2(a))^2$, comparing separately day time and night time climatologies, studied at the three impact altitudes 70 km, 60 km, and 50 km. The time series plots show a clear increase of the quantity $(\alpha_1(a) - \alpha_2(a))^2$ in the years of high solar activity (2001, 2002 and 2011, 2012) and a decrease in the years of low solar activity (2007, 2008). Furthermore the magnitude of the quantity depends on the latitude zone, the season, and also day and night time conditions. Magnitudes decrease towards high latitudes, towards winter conditions, and from day to night time. Obviously also for night time conditions remaining ionization effects cause a residual bias. It is to notice that the $(\alpha_1(a) - \alpha_2(a))^2$ term shows a clear temporal dependance correlated to the solar activity. Furthermore the quantity is a rather stable function with no large irregular fluctuations, except the results found at night time high latitude conditions. The fact that noise does not seem to have a large impact on the temporal term of the model, i.e., $(\alpha_1(a) - \alpha_2(a))^2$, is an advantage of this particular ionospheric correction approach.

As a next step, in Fig. 5.2 the residual ionospheric error ($\Delta\alpha$) is estimated from the relation $\Delta\alpha = -\kappa(\alpha_1(a) - \alpha_2(a))^2$, comparing the value $\kappa(a) = 14\,\mathrm{rad}^{-1}$ to the value $\kappa(a) = 30\,\mathrm{rad}^{-1}$ and using 30° zonal monthly climatologies of $(\alpha_1(a) - \alpha_2(a))^2$ (see also the previous study). As one can see, the magnitude of the residual is driven by the coefficient κ, which makes it so crucial to investigate its latitudinal dependance in simulation studies. Many studies tried to quantify the residual ionospheric error in GPS RO data [e.g., 21, 15, 13, 3, 14], however the error characterization is difficult and the spatial dependance of the error is not completely understood. The hope is to gain information about the spatial dependance of κ from simulation studies. Then observational GPS RO climatologies can get corrected for their residual ionospheric error, using information from the observations itself, i.e., $(\alpha_1(a) - \alpha_2(a))^2$, as well as κ from simulations.

5.2 Correlation to solar activity

As a further investigation the correlation of the $(\alpha_1 - \alpha_2)^2$ term to the solar activity is studied. Since the assumption is that $(\alpha_1 - \alpha_2)^2$ catches the temporal evolution of the sun (~11-years solar cycle), a strong correlation leading to a linear dependance is expected.

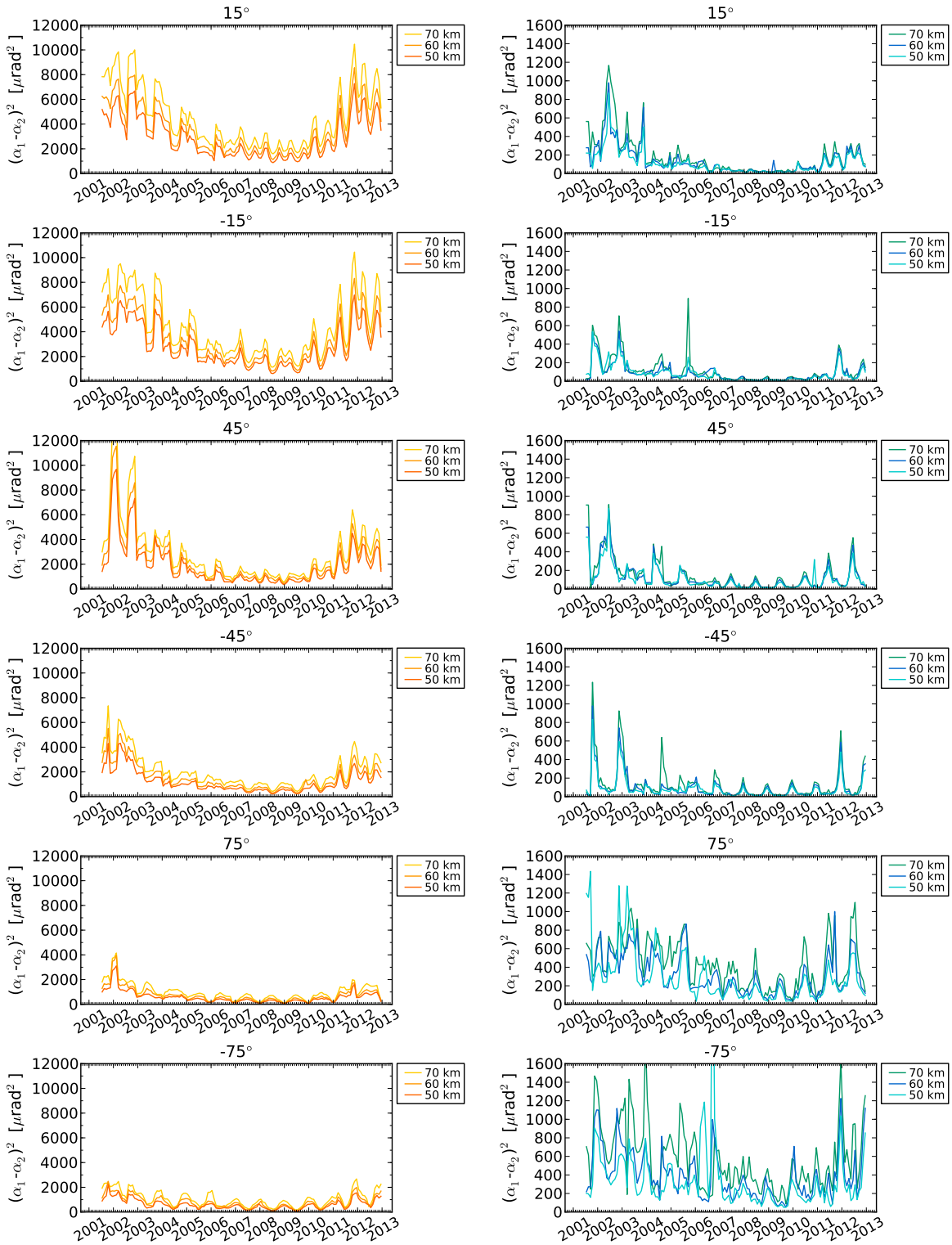

Figure 5.1: *Time series of* $(\alpha_1 - \alpha_2)^2$*, studied for day time (l.h.s.) and night time (r.h.s.)* 30° *zonal monthly mean satellite data on three different impact altitudes.*

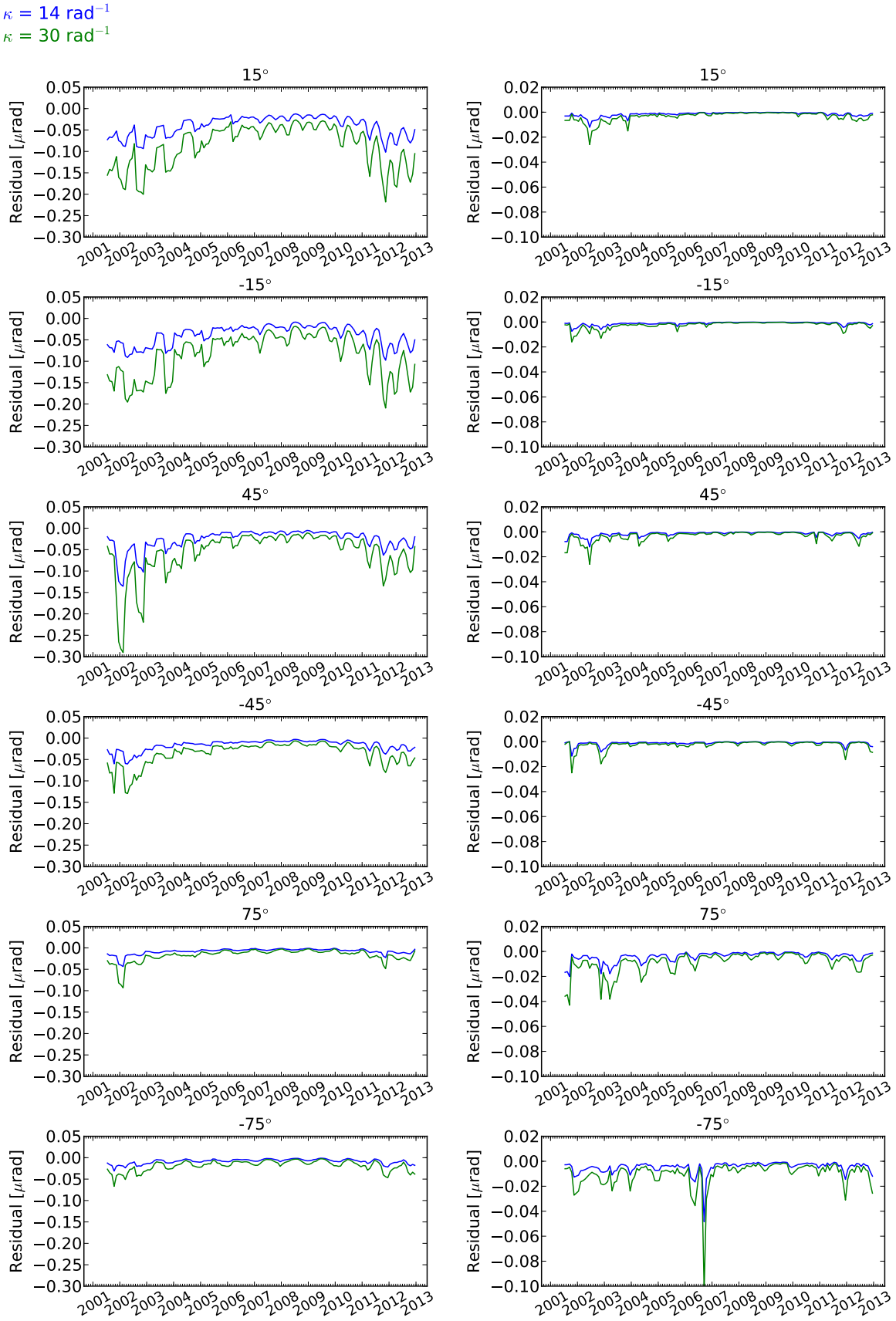

Figure 5.2: *Time series of day time (l.h.s.) and night time (r.h.s.) ionospheric residual, estimated for two values of κ, using 30° zonal monthly mean satellite data at impact altitude* 50 km.

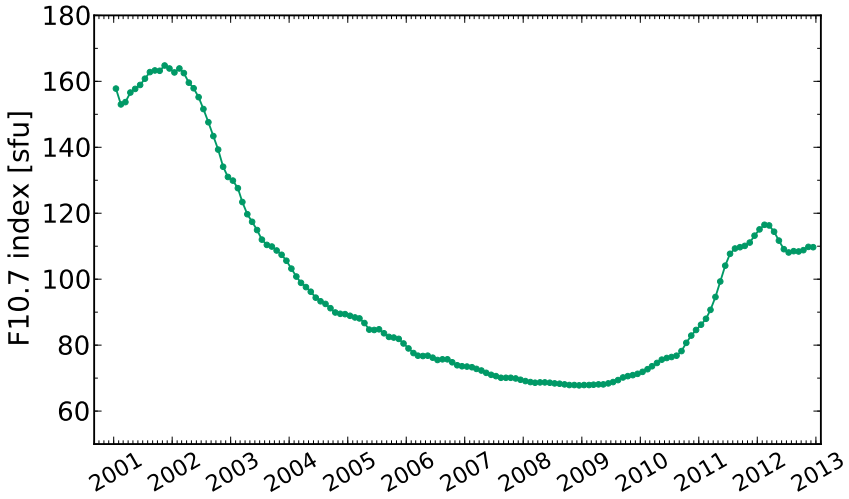

Figure 5.3: *Monthly mean solar radio flux ($F_{10.7}$ index).*

First of all, in Fig. 5.3 the solar activity is plotted dependent on time, using the $F_{10.7}$ index as the measurement observable. Data is taken from the website of the Industrial Plant & Service (IPS) Australia, which provides a smoothed monthly data set. The $F_{10.7}$ index measures the solar radio flux per unit frequency at a wavelength of 10.7 cm. It is given in sfu (1 sfu = $10^{-22}\mathrm{Wm}^{-1}\mathrm{Hz}^{-1}$). The period from 2001 until the end of 2012 involves already two cycle maxima (2001, 2002 and 2011, 2012) and also the minimum years (2007, 2008, 2009).

Comparing Fig. 5.1 with Fig. 5.3 already suggests a correlation between the two quantities. However, since $(\alpha_1 - \alpha_2)^2$ is a quantity dependent on solar cycle, season, and latitude (neglecting the dependance on impact altitude) and the $F_{10.7}$ index depends only on the solar cycle, perfect correlation can not be expected. For this reason I correlated the two quantities separately for each month in order to get rid of the seasonal dependance. Fig. 5.4 studies the monthly day time and night time correlation at impact altitude 50 km. One can observe a positive correlation between the solar activity and the $(\alpha_1 - \alpha_2)^2$ term, however, there exist also large outliers. There are several reasons for that. First of all, the measurements itself contain errors (RO data sets, $F_{10.7}$ data sets). Secondly, smoothed $F_{10.7}$ data was used. For example, the website of NOAA provided until the year 2012 daily $F_{10.7}$ data. Calculating the monthly average of the daily NOAA $F_{10.7}$ data leads to a stronger fluctuating monthly solar cycle with values up to about 240 sfu in the maximum year 2001, compared to the smoothed values of IPS. Finally, always the same solar cycle data set was correlated with different data sets of $(\alpha_1 - \alpha_2)^2$, i.e., data sets dependent on season, latitude, and in our case, also time of day. Despite all these limiting reasons for perfect correlation, a clear dependance between the two quantities could be detected.

As a last plot in this study I show in Fig. 5.5 for 30° zonal observational GPS RO data the possible residual ionospheric error, for different values of κ. The error is correlated with the $F_{10.7}$ index and studied for the month July at the two low latitude bands 15° and −15°. The residual error is defined as $-\kappa(\alpha_1(a) - \alpha_2(a))^2$. It shows a clear linear dependance on the solar activity, where the magnitude of the residual error increases with increasing κ.

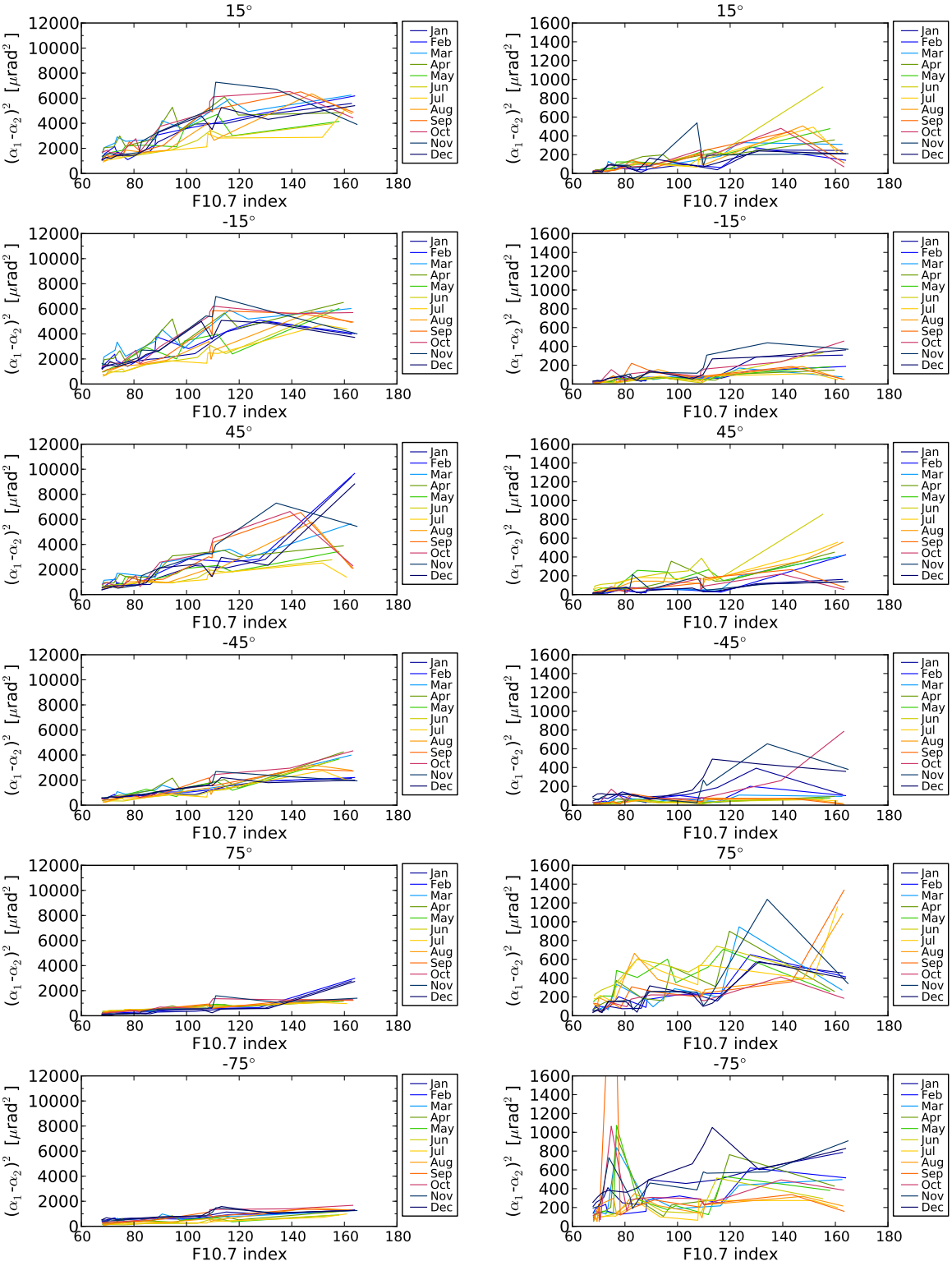

Figure 5.4: *Correlation of* $(\alpha_1 - \alpha_2)^2$ *with* $F_{10.7}$ *index, for day time (l.h.s.) and night time (r.h.s.) satellite data at impact altitude* 50 km*, studied separately for all months.*

Fig. 5.4 and Fig. 5.5 confirmed also for the case of observational GPS RO data that the dependance of the residual ionospheric error on the solar cycle is at least partly captured by the $(\alpha_1 - \alpha_2)^2$ term. The magnitude of the correction depends on the coefficient κ. Since at that point of the study I was not able to determine the latitudinal dependance of κ, no correction on the observational climatologies will be applied. I close the observational data analysis with the conclusion that the approach seems to be very promising, and refer to Sec. 6 for the final discussion.

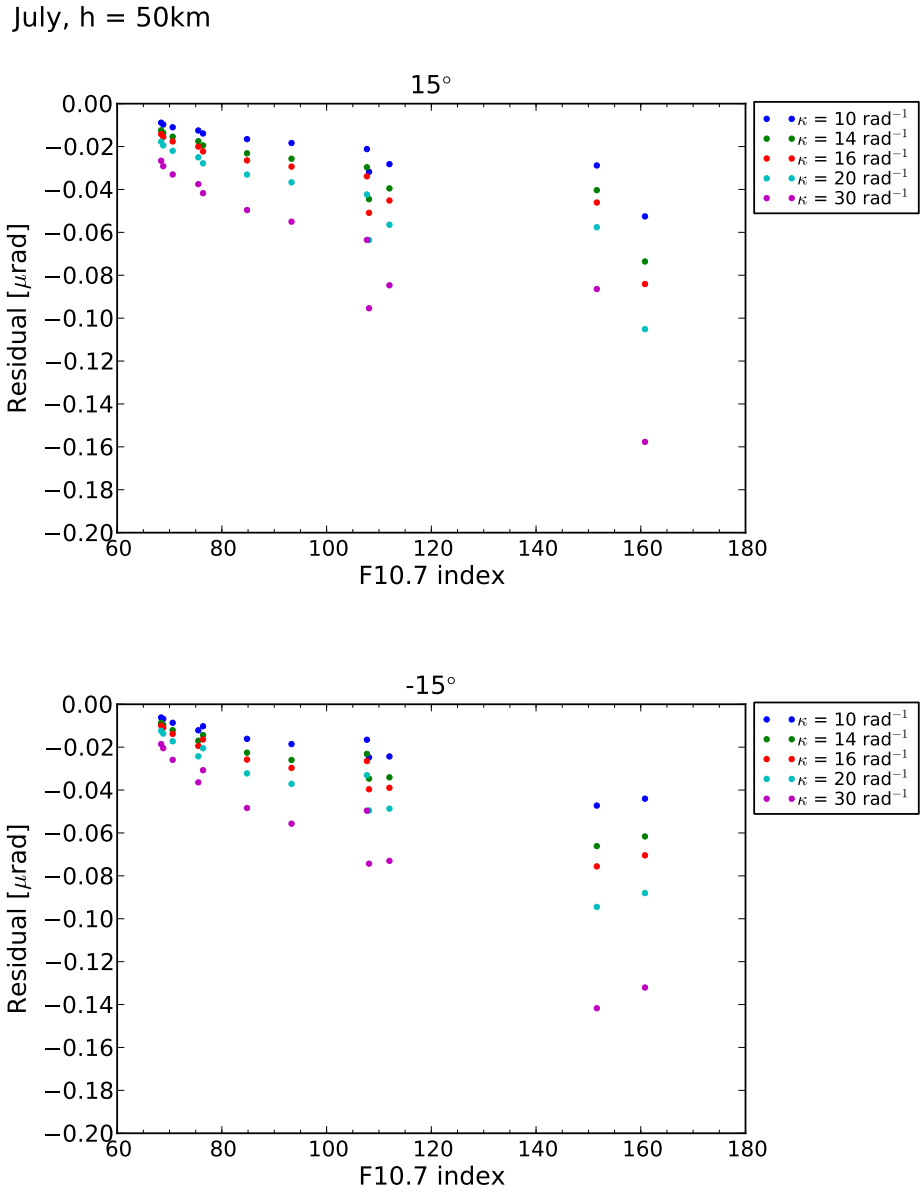

Figure 5.5: *Correlation of day time ionospheric residual with $F_{10.7}$ index, estimated for different values of kappa, studied for satellite data at impact altitude* 50 km *in the month July.*

6 Summary, discussion and outlook

Residual ionospheric errors are a topic of major concern in GPS RO data. Tests showed that at bending angle level and 30 km altitude residual errors of the order of about 0.05 μrad, add an error of about 0.5 K in temperature (e.g., studies Rocken et al. [16, 17], Schreiner et al. [18]). Various first order ionospheric corrections reduce the ionospheric error, but studies showed that residual errors are still a problem, see e.g., Mannucci et al. [15], Liu et al. [13], Danzer et al. [3], Liu et al. [14].

In this study a new model for the residual ionospheric error was introduced and tested. In a first attempt the model was analyzed in a simulation study, in a second attempt it was applied to real observational GPS RO data. The model itself is based on the bending angles $\alpha_1(a)$ and $\alpha_2(a)$, and the coefficient $\kappa(a)$, where a is the dependance on impact altitude. Basically the model is constructed out of two terms: A temporal term, given by the difference of the bending angles α_1 and α_2 squared, and a time constant term $\kappa(a)$. The temporal term depends on the solar activity, i.e., the state of the ionosphere, increasing and decreasing with the solar cycle. It is assumed to catch the temporal evolution of the residual ionospheric error. The time constant factor $\kappa(a)$ is related to the magnitude of the residual ionospheric error, which depends on season and geographic location.

In the first part of the analysis I simulated globally day and night time bending angle profiles for the month January, from 2001 until 2011, with and without ionosphere, using the NeUoG model for simulating the non-spherical ionosphere. The NeUoG model is driven by the $F_{10.7}$ index and the profiles simulated with ionosphere were modeled according to the solar cycle in this period of time, using observational $F_{10.7}$ data. Extremely noisy bending angles with values larger or smaller than $\pm 7\,\mu$rad in an altitude range between 50 km to 80 km were rejected as outliers.

In the simulation study it was possible to investigate the residual ionospheric error directly as the difference between a bending angle profile simulated with ionosphere and the co-located neutral atmospheric bending angle profile. Furthermore, the residual error could be studied from the proposed error model. One of the main goals was to see if the temporal term of the model catches the temporal behavior of the residual ionospheric error. Since the residual error is a very small number (less than about 0.3 μrad) and the noise of the data was in the same order of magnitude, it was difficult to study correlation. Hence, I decided to perform a vertical smoothing of the data, by averaging over ± 2.5 km from above to below the studied impact altitude. After having performed the vertical smoothing step of the data, it was possible to detect a clear correlation signal between the residual ionospheric error and the temporal term of the model, at least at low latitudes. At mid to high latitudes the noise of the simulated data was still a remaining problem. From the correlation study, $\kappa(a)$ could be calculated as the coefficient of the linear fit. It was found to be at low latitudes in the same range of values as obtained from one-dimensional Chapman layer calculations, which is about $\kappa(a) = 14\,\mathrm{rad}^{-1}$, being relatively constant with impact altitude.

Finally, a first attempt of correcting bending angle data with the proposed error model was conducted. Tested for the latitude band 0°, temperature profiles simulated with ionosphere were studied as a difference to the co-located neutral atmospheric temperature profiles. This temperature difference was analyzed for profiles where no ionospheric correction was applied and for profiles were the model correction was applied. Clearly, when applying the residual ionospheric correction, the difference to the neutral atmospheric profiles reduced, i.e., the residual influence of the ionosphere got smaller, which is a very encouraging result.

The study with observational satellite data was performed in the time period from 2001 to 2012, using bending angle data from the CHAMP and COSMIC satellite missions. The temporal term of the proposed residual error model, which contains only the two GPS RO quantities α_1 and α_2, was studied for 30° zonal climatologies. A very distinct increase of the magnitude of the studied temporal model term in times of high solar activity, and decrease in times of low solar activity, could be observed. In general, the advantage of the temporal model term is that it is between 50 km to 70 km impact altitude in the order of between about $1000\,\mu\text{rad}^2$ to $12\,000\,\mu\text{rad}^2$, depending on latitude, season, and solar activity. Due to these large magnitudes noise does not play a significant role, leading to a rather clean time dependent correction function. Correlating the temporal model term with the solar activity and using the $F_{10.7}$ index as tracer for the solar activity, indicated a positive correlation, however with large fluctuations. For that several explanations exist: Possible measurement errors, the usage of smoothed $F_{10.7}$ data, and most importantly, the temporal model term depends on latitude, season, and solar activity, while the $F_{10.7}$ index depends only on the solar activity. Despite these limiting reasons for a very strong linear correlation it could be shown that the two functions correlate and that the temporal model term will probably correct for the temporal dependance of the residual ionospheric error. However, the magnitude for the correction of the residual error depends on the coefficient κ.

This already leads over to the discussion part. In order to be able to apply the proposed residual ionospheric error model it is crucial to determine the spatial dependance of the coefficient κ. In this study it was the goal to perform a thorough spatial investigation of κ in the simulation study. However, it was not possible to study κ at mid to high latitudes due to large fluctuations of the bending angle profiles which were simulated with ionosphere. The problem is that the determination of κ through a linear fit requires on the one hand the study of the bending angle difference between profiles simulated with ionosphere and the co-located neutral atmosphere profiles, i.e., the residual ionospheric error, and it requires on the other hand the determination of the temporal model term. While the temporal model term is, as mentioned, a quantity with a large magnitude and therefore rather unaffected from noise, the residual error is a very small number, where noise automatically plays a significant role. This leads to sometimes large fluctuations which affects the determination of κ.

In order to be able to perform a thorough latitudinal investigation of the coefficient κ I suggest to repeat the simulation study and produce a larger ensemble. Studying such small magnitudes needs a large statistics in order to reduce noise. Furthermore, there is the goal to perform improvements in the NeUoG model, since there exist some known problems in the ray tracing procedure. Maybe with the larger ensemble and the improvements in the ray tracing it will be possible to determine κ also at mid and high latitudes. As another idea, there exists also the possibility to study the coefficient κ from a different perspective. The idea is to also use MIPAS (Michaelson Interferometer for Passive Atmospheric Sounding) and SABER (Sounding of the Atmosphere using Broadband Emission Radiometry) data, which is currently prepared and validated at the WEGC against GPS RO data, for the residual ionospheric error study. The MIPAS and SABER instruments provide high quality data also up to altitudes of 80 km. One could retrieve the residual ionospheric error by studying GPS RO bending angle climatologies against co-located MIPAS and SABER bending angle climatologies. As a next step the correlation of the retrieved residual ionospheric error with the temporal model term could be studied in order to determine the coefficient κ from a linear fit. The results can then be compared to the results from the repeated simulation study.

As a concluding remark there is to mention that the proposed residual error model is probably mainly suited for performing a bending angle correction on bending angle climatologies, i.e., it is understood as a climatological correction, instead of applying it on single bending angle profiles. The reason is that the coefficient $\kappa(a)$ needs to be determined for this correction, which is probably only possible to conduct in a climatological sense, and not for single profiles. Only if the coefficient is found to be very insensitive with latitude and longitude I assume that it could be applied also to single profiles. Recently, it has been proposed for climatological studies with GPS RO data to perform the averaging of the atmospheric parameters already in bending angle space [1, 6, 2, 4]. This avoids the usage of a priori information in the data through a complicated statistical optimization step, which was detected to be a major error source between the main processing centers of GPS RO data [8, 20]. Using observational bending angle climatologies up to an altitude of 80 km requires also to take the residual influence of the ionosphere in the satellite data into account. The residual ionospheric error model would be highly suited for this specific approach of climatological studies.

Summarized, this study showed some very encouraging first results in the simulation study, as well as satellite data study, supporting the residual ionospheric error model. Although a thorough latitudinal investigation of the coefficient κ was not possible, it became clear from this work to further engage in the study of the proposed model.

Acknowledgments

I would like to thank Sean Healy and Ian Culverwell for letting me be part of this very interesting work. Especially I want to thank Sean Healy from whom I learned a lot through his always critical questions and the lively discussions. Furthermore I acknowledge ROM SAF for providing the possibility of this visiting scientist activity. Finally, I thank the Wegener Center which provided the processing and simulation software, and especially Gottfried Kirchengast, for his support and the discussions about the ionosphere model.

6.1 Acronyms and abbreviations

CDAAC	Cosmic Data Analysis and Archive Center
CLIPS2	Climatology Processing System 2
DMI	Danish Meteorological Institute (ROM SAF Leading Entity)
ECMWF	The European Centre for Medium-Range Weather Forecasts
EGOPS	End-to-End Generic Occultation Performance and Processing System
EUMETSAT	European Organisation for the Exploitation of Meteorological Satellites
CHAMP	Challenging Mini–Satellite Payload
COSMIC	Constellation Observing System for Meteorology
GPS	Global Positioning System (US)
IPS	Industrial Plant & Service
Met Office	United Kingdom Meteorological Office
MIPAS	Michaelson Interferometer for Passive Atmospheric Sounding
MSIS	Mass Spectrometer and Incoherent Scatter Radar
RO	Radio Occultation
ROM SAF	Radio Occultation Meteorology SAF (former GRAS SAF)
SABER	Sounding of the Atmosphere using Broadband Emission Radiometry
SAF	Satellite Application Facility (EUMETSAT)
UCAR	University Corporation for Atmospheric Research
UTLS	Upper Troposphere and Lower Stratosphere
WEGC	Wegener Center for Climate and Global Change

Bibliography

[1] Ao, C. O., Mannucci, A. J., and Kursinski, E. R.: Improving GPS Radio Occultation Stratospheric Refractivity Retrievals for Climate Benchmarking, Geophysical Research Letters, 39, doi:10.1029/2012GL051720, 2012.

[2] Danzer, J.: Feasibility of generating long-term RO refractivity climatologies without using statistical optimization, Tech. rep., ROM SAF, CDOP-2 Visiting Scientist Report 23, Ref: SAF/ROM/DMI/REP/VS/23, http://www.romsaf.org, 2014.

[3] Danzer, J., Scherllin-Pirscher, B., and Foelsche, U.: Systematic residual ionospheric errors in radio occultation data and a potential way to minimize them, Atmospheric Measurement Techniques, 6, 2169–2179, doi:10.5194/amt-6-2169-2013, URL `http://www.atmos-meas-tech.net/6/2169/2013/`, 2013.

[4] Danzer, J., Gleisner, H., and Healy, S.: CHAMP climate data based on inversion of monthly average bending angles, Atmospheric Measurement Techniques Discussions, 7, 7811–7835, 2014.

[5] Fritzer, J., Kirchengast, G., and Pock, M.: End-to-End Generic Occultation Performance Simulation and Processing System Version 5.5 (EGOPS5.5) Software User Manual, Tech. rep., University of Graz, Austria, WEGC and IGAM, WEGC–EGOPS–2009–TR01, 2009.

[6] Gleisner, H. and Healy, S. B.: A simplified approach for generating GNSS radio occultation refractivity climatologies, Atmospheric Measurement Techniques, 6, 121–129, doi:10.5194/amt-6-121-2013, URL `http://www.atmos-meas-tech.net/6/121/2013/`, 2013.

[7] Healy, S. B. and Culverwell, I.: personal communication, 2014.

[8] Ho, S.-P., Hunt, D., Steiner, A. K., Mannucci, A. J., Kirchengast, G., Gleisner, H., Heise, S., von Engeln, A., Marquardt, C., Sokolovskiy, S., Schreiner, W., Scherllin-Pirscher, B., Ao, C., Wickert, J., Syndergaard, S., Lauritsen, K. B., Leroy, S., Kursinski, E. R., Kuo, Y.-H., Foelsche, U., Schmidt, T., and Gorbunov, M.: Reproducibility of GPS radio occultation data for climate monitoring: Profile-to-profile inter-comparison of CHAMP climate records 2002 to 2008 from six data centers, Journal of Geophysical Research, 117, D18 111, doi:10.1029/2012JD017665, 2012.

[9] Kursinski, E. R., Hajj, G. A., Schofield, J. T., Linfield, R. P., and Hardy, K. R.: Observing Earth's atmosphere with radio occultation measurements using the Global Positioning System, Journal of Geophysical Research, 102, D19, 1997.

[10] Ladreiter, H. P. and Kirchengast, G.: GPS/GLONASS sensing of the neutral atmosphere: Model-independent correction of ionospheric influences, Radio Sci., 31, 877–891, doi:10.1029/96RS01094, 1996.

[11] Leitinger, R. and Kirchengast, G.: Easy to use global and regional models - A report on approaches used in Graz, Acta Geod. Geophys. Hung., 32, 329–342, 1997.

[12] Leitinger, R., Titheridge, J. E., Kirchengast, G., and Rothleitner, W.: A "simple" global empirical model for the F layer of the ionosphere, Tech. rep., University Graz, 1995.

[13] Liu, C., Kirchengast, G., Zhang, K., Norman, R., Li, Y., Zhang, S., Carter, B., Fritzer, J., Schwaerz, M., Choy, S., et al.: Characterisation of residual ionospheric errors in bending angles using GNSS RO end-to-end simulations, Advances in Space Research, 52, 821–836, 2013.

[14] Liu, C. L., Kirchengast, G., Zhang, K. F., Norman, R., Li, Y., Zhang, S. C., Fritzer, J., Schwaerz, M., Wu, S. Q., and Tan, Z. X.: Quantifying residual ionospheric errors in GNSS radio occultation bending angles based on ensembles of profiles from end-to-end simulations, paper in preparation, 2014.

[15] Mannucci, A. J., Ao, C. O., Pi, X., and Iijima, B. A.: The impact of large scale ionospheric structure on radio occultation retrievals, Atmospheric Measurement Techniques, 4, 2837–2850, doi:10.5194/amt-4-2837-2011, URL http://www.atmos-meas-tech.net/4/2837/2011/, 2011.

[16] Rocken, C., Schreiner, B., Sokolovskiy, S., Hunt, D., and Syndergaard, S.: Formosat3/COSMIC, the Ionosphere as Signal and Noise, Space Weather Workshop, 2008.

[17] Rocken, C., Schreiner, W., Sokolovskiy, S., and Hunt, D.: Ionospheric errors in COSMIC radio occultation data, paper presented at the 89th American Meteorological Society Annual Meeting, 2009.

[18] Schreiner, B., Sokolovskiy, S., Hunt, D., Ho, B., and Kuo, B.: Use of GNSS Radio Occultation data for Climate Applications, presentation at the World Climate Research Programme (WCRP) workshop, 2011.

[19] Spilker, J. J.: Signal Structure and Performance Characteristics, in: Janiczek, P.M. (ed.), Global Positioning System: Papers Published in NAVIGATION, 1, 29–54, 1980.

[20] Steiner, A. K., Hunt, D., Ho, S.-P., Kirchengast, G., Mannucci, A. J., Scherllin-Pirscher, B., Gleisner, H., von Engeln, A., Schmidt, T., Ao, C., Leroy, S. S., Kursinski, E. R., Foelsche, U., Gorbunov, M., Heise, S., Kuo, Y.-H., Lauritsen, K. B., Marquardt, C., Rocken, C., Schreiner, W., Sokolovskiy, S., Syndergaard, S., and Wickert, J.: Quantification of structural uncertainty in climate data records from GPS radio occultation, Atmospheric Chemistry and Physics, 13, 1469–1484, doi:10.5194/acp-13-1469-2013, URL http://www.atmos-chem-phys.net/13/1469/2013/, 2013.

[21] Syndergaard, S.: On the ionosphere calibration in GPS radio occultation measurements, Radio Science, 35, 865–883, 2000.

[22] Vorob'ev, V. V. and Krasil'nikova, T. G.: Estimation of the accuracy of the atmospheric refractive index recovery from Doppler shift measurements at frequencies used in the NAVSTAR system, Izvestiya, Atmospheric and Oceanic Physics, 29, 602–609, 1994.